Magnetic Reconnection in strongly magnetized regions around the Solar TMR —Multi-fluid Simulations

Lei Ni

Yunnan Observatories, China

Collaborators: Vyacheslav (Slava) Lukin (NSF, USA)

Nicholas A. Murphy(CfA, USA)

Jun Lin (Yunnan Observatories, China)

IRIS9, Gottingen, Germany

26/06/2018

IRIS-9, Göttingen, 25-29 June 2018

Invited Talk

1. Fundamental physical processes and modeling

Magnetic reconnection in strongly magnetized regions around the solar TMR

Lei Ni

Yunnan Observatories, China

Magnetic reconnection (MR) is the most likely mechanism responsible for the high temperature events that are frequently observed around the solar TMR. We have studied MR in such an environment by employing MHD-based simulations of a partially ionized plasma within a reactive 2.5D multi-fluid model. In strongly magnetized regions with low plasma β, the initially weakly ionized plasmas become strongly ionized during the MR process and the ionized and neutral fluid flows are well-coupled throughout the reconnection region. The reconnection characteristics are then close to those in fully ionized plasmas, the reconnection process resembles the Sweet-Parker model before magnetic islands appear, and the plasmoid instability is the main physical mechanism to result in the fast magnetic reconnection in a high Lundquist number MR process. Decoupling of the ion and neutral inflows appears obviously in a high β case, and we observe MR much faster than the single-fluid Sweet-Parker prediction. The rate of ionization of the neutral component of the plasma is always faster than recombination within the current sheet region even when the initial plasma β is as high as $\beta = 1.46$. The non-equilibrium ionization-recombination dynamics play a critical role in determining the structure of the reconnection region, lead to much lower temperature increases as compared to simulations that assume plasma to be in ionization-recombination equilibrium. However, the plasma temperature increases with time inside the current sheet, we can still find that the maximum value is above 20000 K when the reconnection magnetic field strength is greater than 500 G. Therefore, the Si IV emission lines can still possibly be produced during such a MR process around the solar TMR.

Magnetic Reconnection in strongly magnetized regions around the Solar TMR —Multi-fluid Simulations

Lei Ni

Yunnan Observatories, China

Collaborators: Vyacheslav (Slava) Lukin (NSF, USA)

Nicholas A. Murphy(CfA, USA)

Jun Lin (Yunnan Observatories, China)

IRIS9, Gottingen, Germany

26/06/2018

OUT LINE

- **1. Background**
- (1) Observations
- (2) Theory and numerical simulations
- **2. Numerical setups and Results**
- **3. Summary and conclusions**
- **4. Future Plans**

Observations

The traditional Ellerman Bombs and IRIS bombs:

(e.g., Li et al 2015; Nelson et al 2015; Pariat et al. 2007;Fang et al 2006; et al 2002)

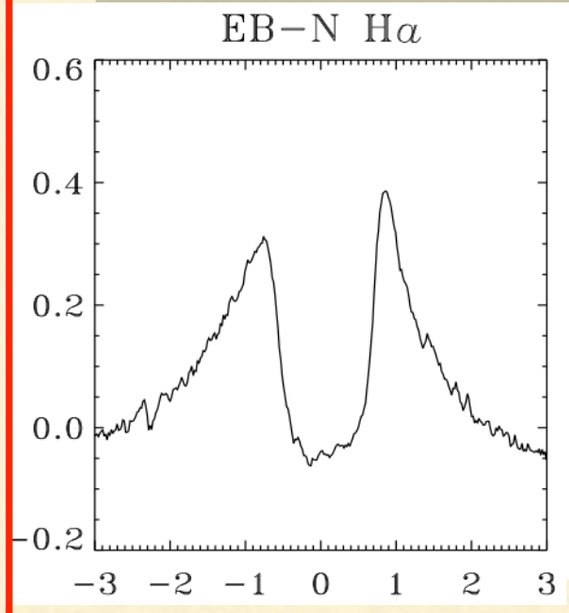

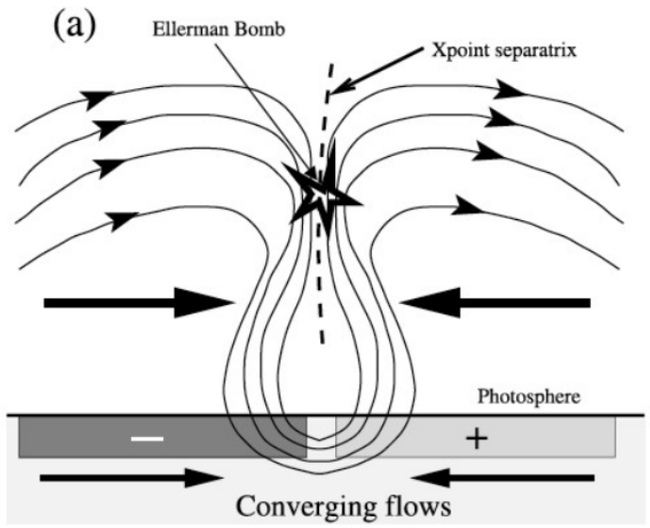

Peter et al 2014, science

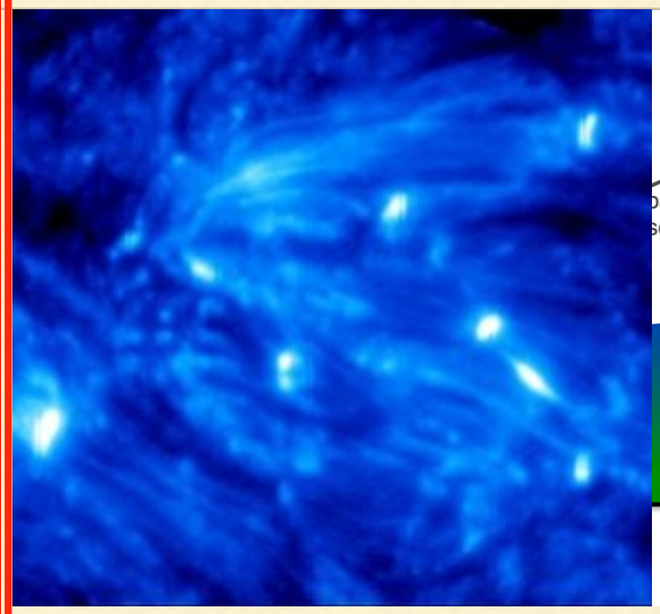

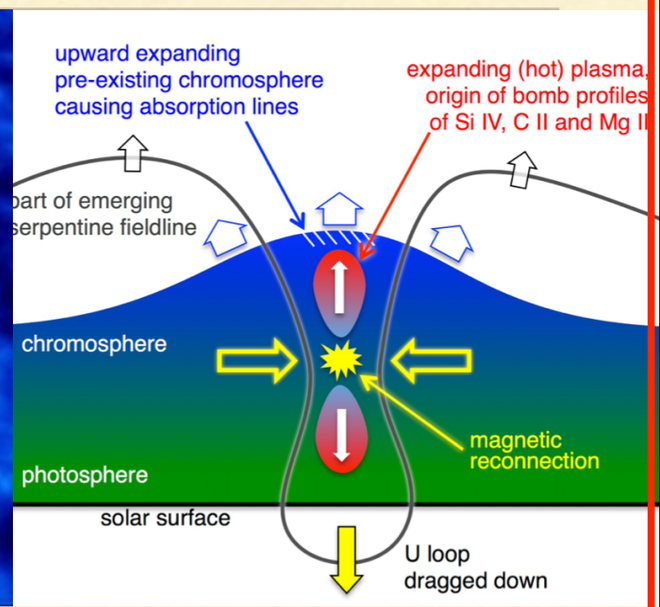

	T increase:	energy :	Size:	durations:
EB	600-3000 K	$5x10^{25}$-$3x10^{26}$ ergs	0.3”-0.8”	3-5 min
IRIS B	~$8x10^4$ K ?	> 10^{27} ergs	0.3”-0.8”	3-5 min

IRIS bombs (UV burst) connect to EBs or not?

Observations

Some EBs and QSEBs are connected to IRIS bombs (UV burst).

(e.g., Vissers et al. 2015; Tian et al. 2016; Nelson et al. 2017; Tian et al. 2018 a)

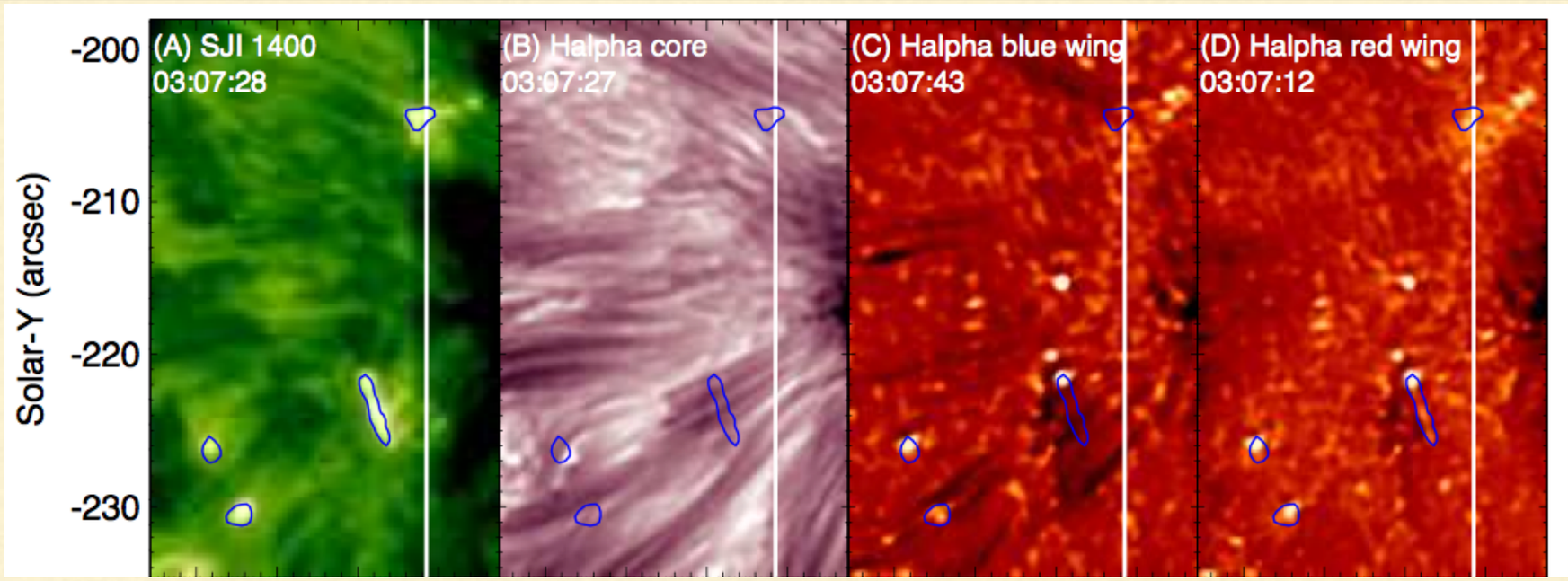

(Tian et al, 2016 APJ) Joint observations Between IRIS and NVST. For 10 IRIS bombs, 3 are definitely connected to EBs, 3 are possible.

Si IV 1394 and 1403 lines → T at least 20,000~K in the dense photosphere

Fe II and Ni II absorption lines → hot MR region below cooler chromosphere

All bursts are located in regions of large squashing factor at the height of ~ 1Mm (Tian et al . 2018 b)

MR happens around solar TMR (~250-1000 km above the solar surface).

The initial high density low temperature plasmas should be heated above 20, 000 K.

Observations

Some EBs and QSEBs are connected to IRIS bombs (UV burst).

(e.g., Vissers et al. 2015; Tian et al. 2016; Nelson et al. 2017; Tian et al. 2018 a)

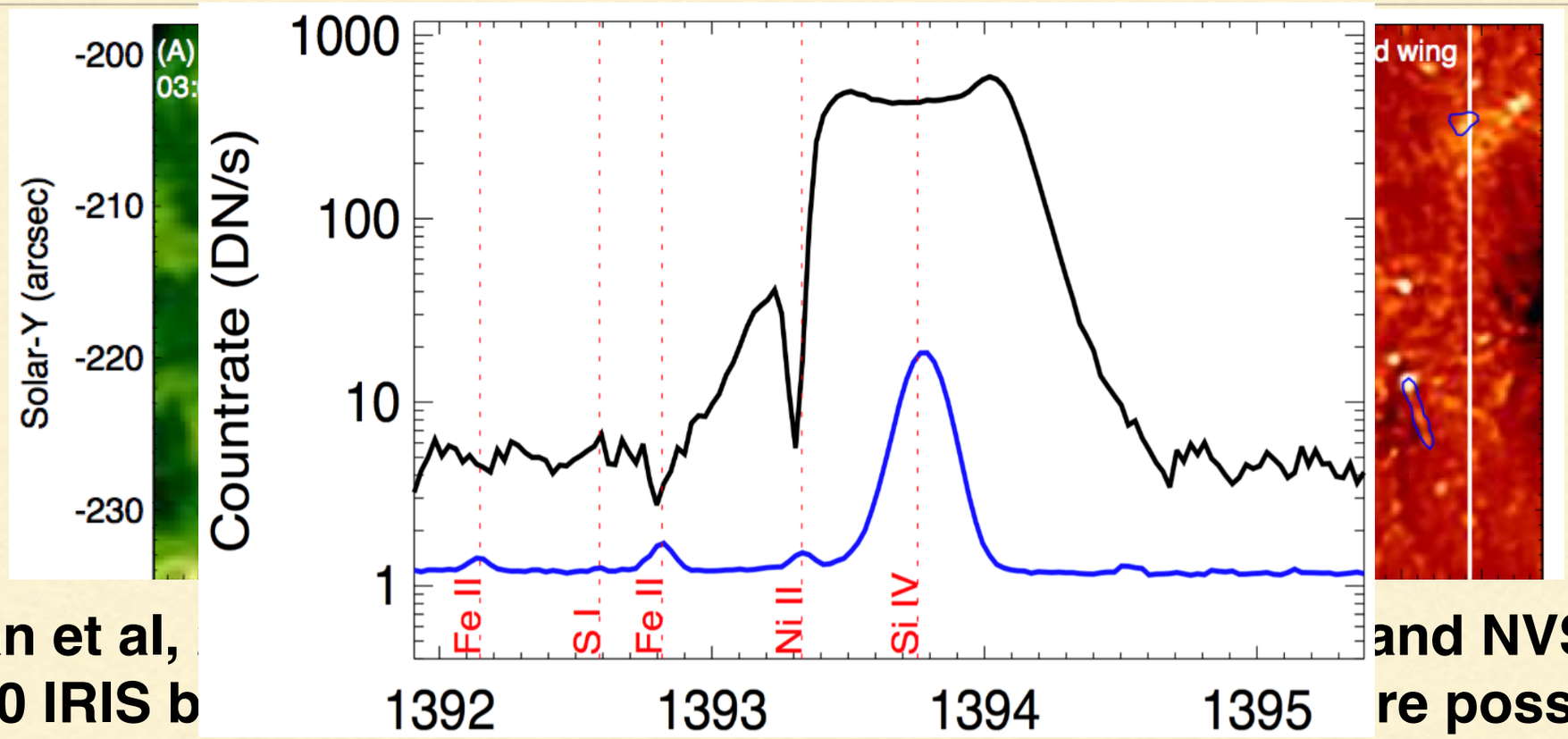

(Tian et al, … and NVST. For 10 IRIS b… re possible.

Si IV 1394 and 1403 lines ⟶ T at least 20,000~K in the dense photosphere

Fe II and Ni II absorption lines ⟶ hot MR region below cooler chromosphere

All bursts are located in regions of large squashing factor at the height of ~ 1Mm (Tian et al . 2018 b)

MR happens around solar TMR (~250-1000 km above the solar surface).

The initial high density low temperature plasmas should be heated above 20, 000 K.

Observations

Some EBs and QSEBs are connected to IRIS bombs (UV burst).

(e.g., Vissers et al. 2015; Tian et al. 2016; Nelson et al. 2017; Tian et al. 2018 a)

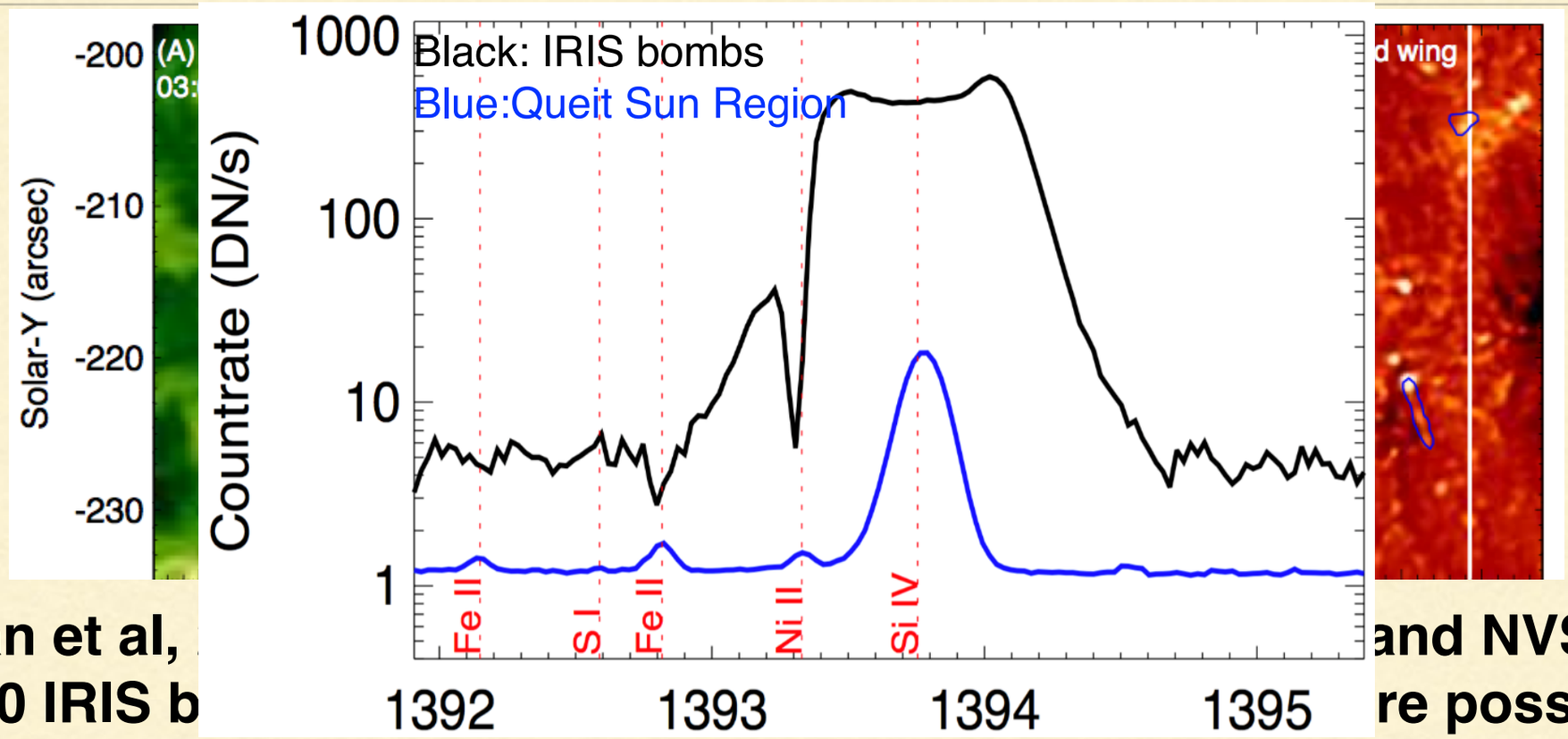

(Tian et al, … and NVST. For 10 IRIS b… re possible.

Si IV 1394 and 1403 lines ⟶ T at least 20,000~K in the dense photosphere

Fe II and Ni II absorption lines ⟶ hot MR region below cooler chromosphere

All bursts are located in regions of large squashing factor at the height of ~ 1Mm (Tian et al . 2018 b)

MR happens around solar TMR (~250-1000 km above the solar surface).

The initial high density low temperature plasmas should be heated above 20, 000 K.

Theory and Numerical simulations

Xu et al 2011

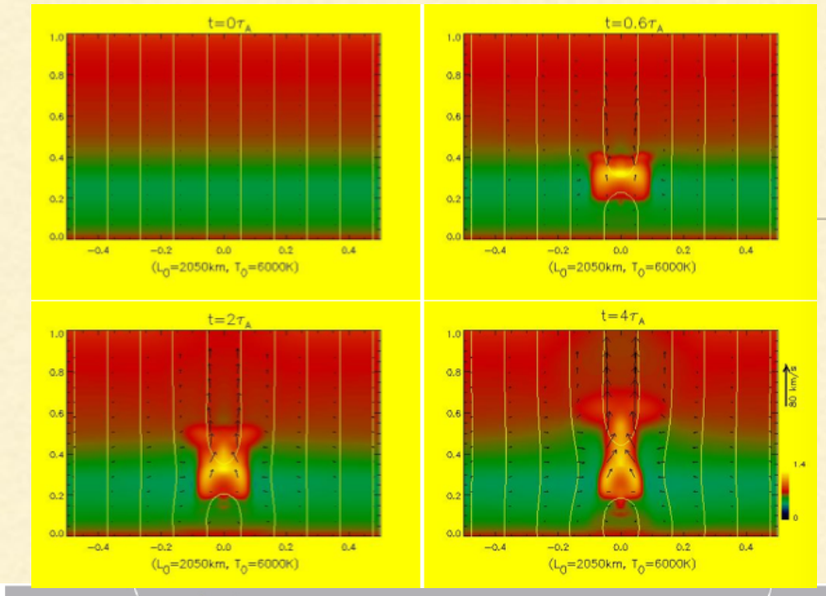

Archontis & Hood 2009

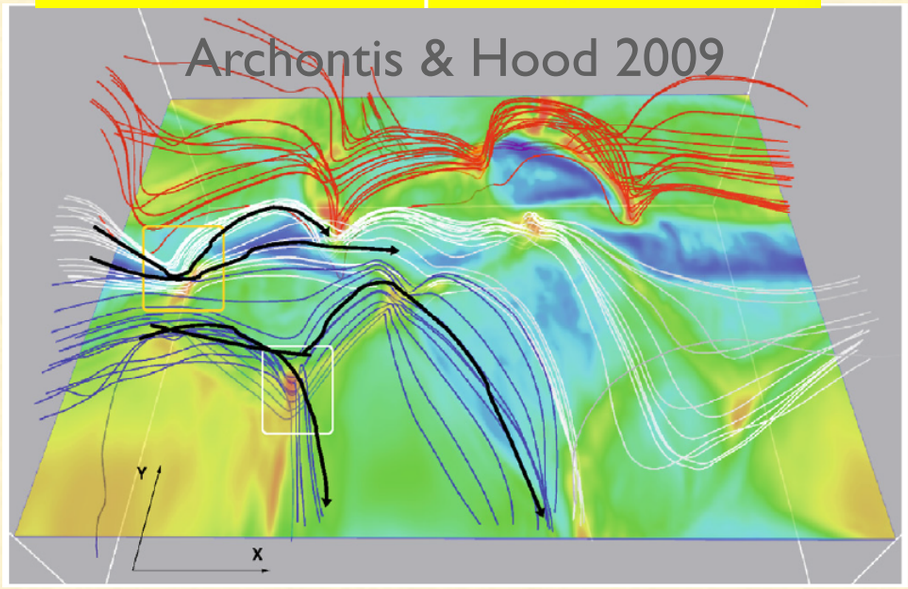

Hansteen et al 2017

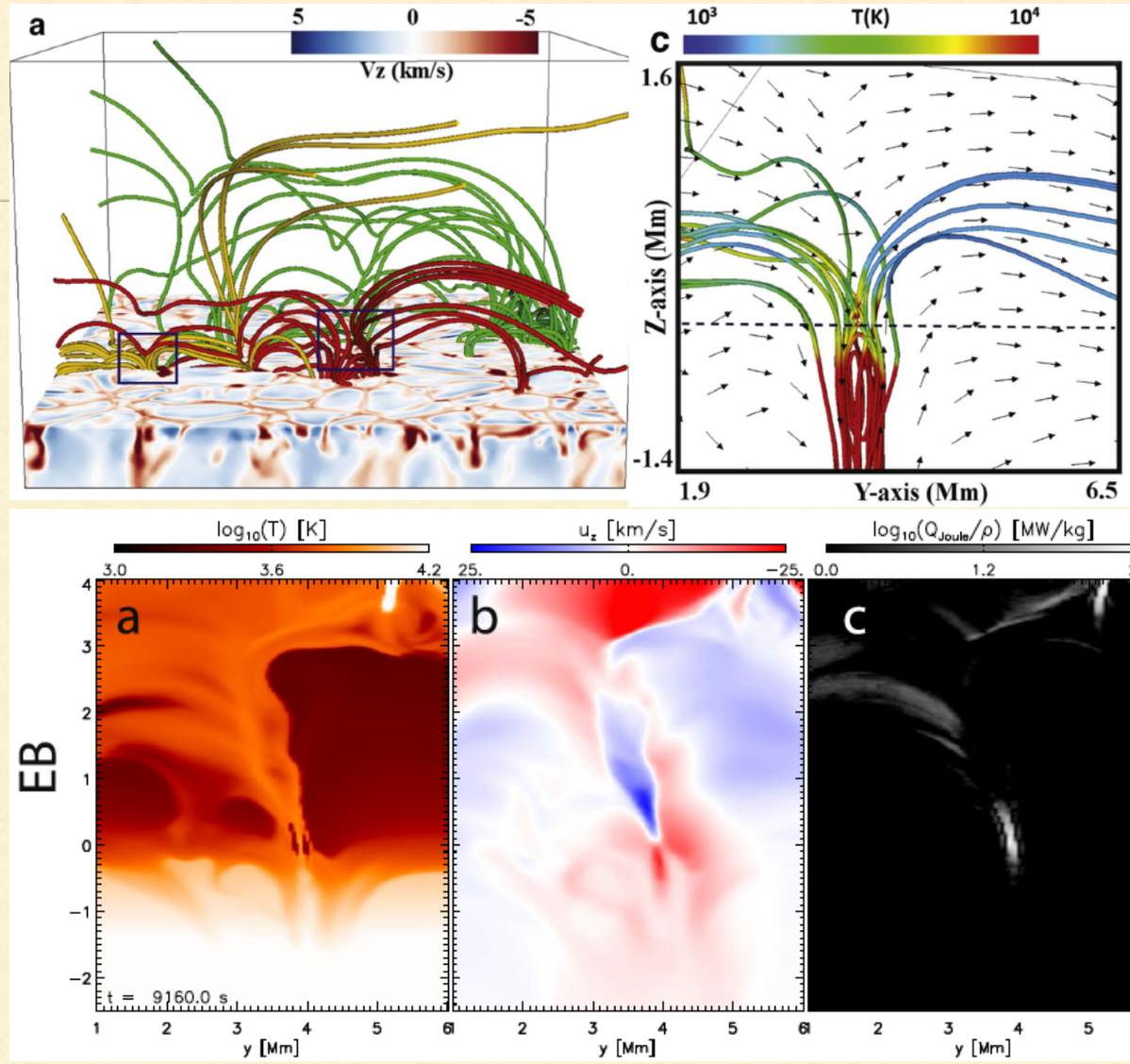

The maximum temperature increase is only about several thousand K.

Problems: one-fluid (ionization-recombination equilibrium), low resolution (Artificial magnetic diffusion, small scale physics ignored), Ambipolar diffusion not included.

Theory and Numerical simulations

Ni et al 2016

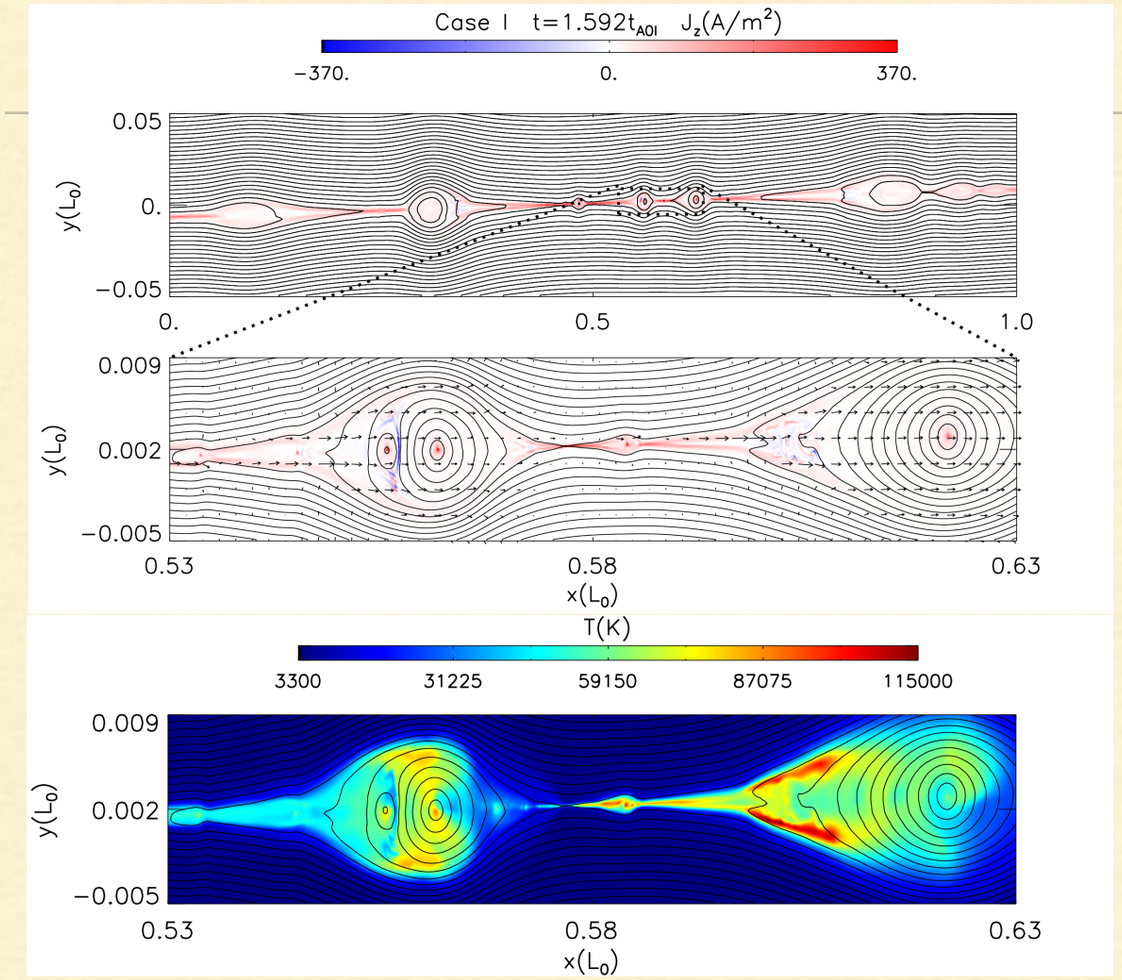

Around TMR(600km), with B_0=500G, β_0=0.058

high resolution (almost realistic magnetic diffusion), ambipolar diffusion, optically thin radiative cooling and heat conduction

Shocks inside the magnetic islands can heat plasma from 4200 K to above 80,000 K

Problems: One-fluid, fixed ionization rate, radiative cooling needs to be modified

Theory and Numerical simulations

- The contributions of neutrals to MR：（1) ionization, recombination and charge exchange; (2) contribution to magnetic diffusion (collisions between electrons and neutrals)；（3)Ambipolar diffusion，neutrals are not coupled with magnetic fields；(Brandenburg & Zweibel 1994,1995;Vishniac & Lazarian 1999; Ni et al 2015);（4）viscous heating by neutrals; (5) heat conduction by neutrals

- Multi-fluid model for MR: Ambipolar diffusion is self-consistently included, non-equilibrium ionization-recombination included, the other interactions between ions and neutrals included, (Leake et al. 2012, 2013; Murphy & Lukin 2015; Alvarez Laguna et al 2017).

- Radiative cooling in MR: simple radiative cooling model (Leake et al. 2012, 2013; Murphy & Lukin 2015), the model calculated by using OPACITY project and CHIANTI databases (Alvarez Laguna et al 2017), solve the radiative transfer equations (Hansteen et al 2017).

Theory and Numerical simulations

- Important conclusions from the Multi-fluid simulations of MR in the middle of solar chromosphere (1000km-1500km above the solar surface, Zero guide field) (Leake et al 2012, 2013; Alvarez Laguna et al 2017):

(1) neutral and ion fluids can become decoupled upstream of the reconnection current sheet but are well-coupled in the outflows;
(2) strong ion recombination in the reconnection region, combined with Alfvénic outflows, lead to a fast reconnection rate independent of Lundquist number;
(3) Plasmoid instability only increases the reconnection rate by 15%.

ion-neutral mean free path: $\lambda_{ni} \sim n_i^{-1}$; neutrals and ions become decoupled only when the current sheet width compares with λ_{ni} , the effect of recombination on MR then becomes obvious.

ion-inertial length: $d_i \sim n_i^{-0.5}$, Hall effect becomes efficient only when the current sheet width compares with d_i .

Theory and Numerical simulations

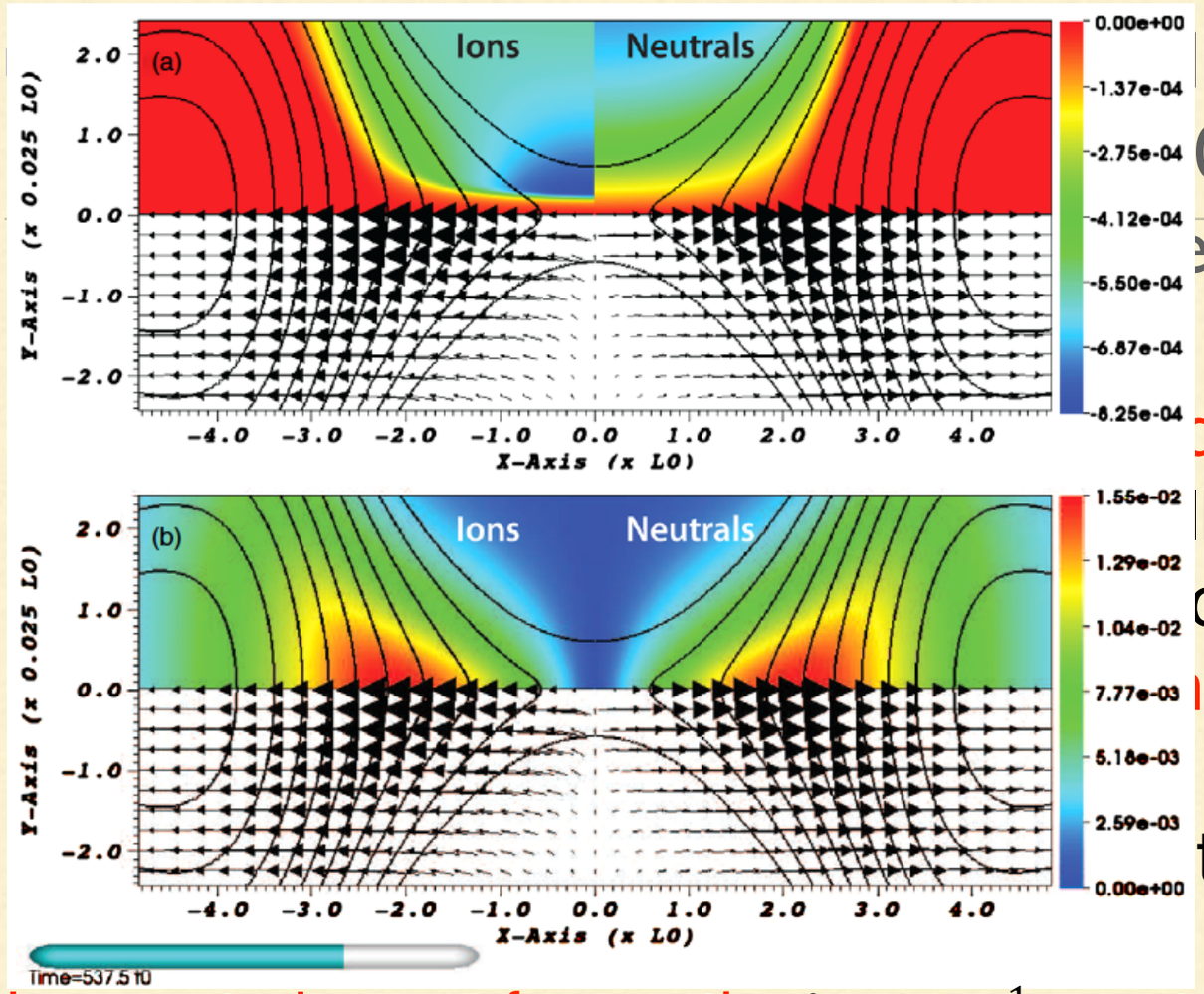

ulti-fluid simulations of MR in the
00km-1500km above the solar
et al 2012, 2013; Alvarez Laguna et al

decoupled upstream of the
l-coupled in the outflows;
onnection region, combined with
nection rate independent of Lundquist

the reconnection rate by 15%.

ion-neutral mean free path: $\lambda_{ni} \sim n_i^{-1}$, neutrals and ions become decoupled only when the current sheet width compares with λ_{ni} , the effect of recombination on MR then becomes obvious.

ion-inertial length: $d_i \sim n_i^{-0.5}$, Hall effect becomes efficient only when the current sheet width compares with d_i .

Theory and Numerical simulations

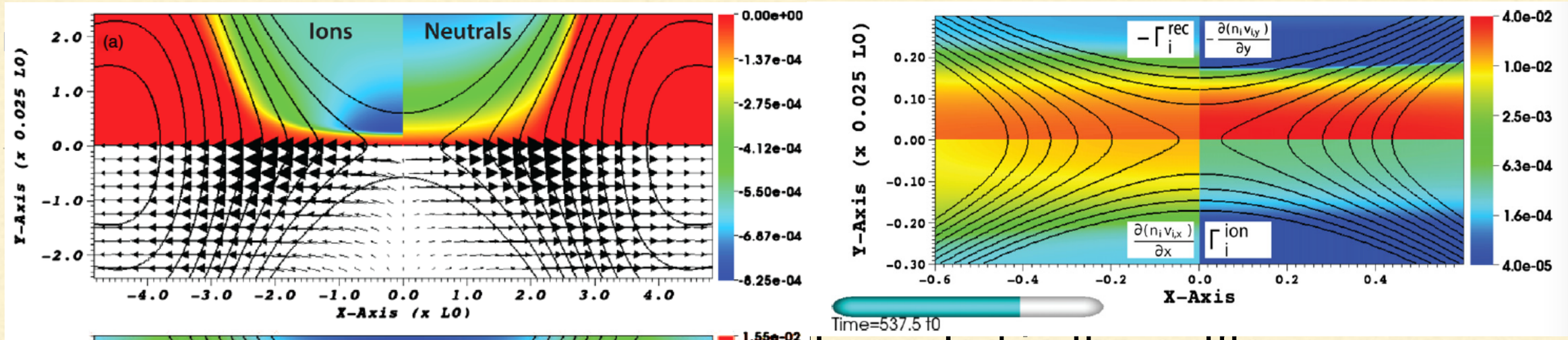

al

l-coupled in the outflows;

onnection region, combined with

ection rate independent of Lundquist

the reconnection rate by 15%.

ion-neutral mean free path: $\lambda_{ni} \sim n_i^{-1}$, neutrals and ions become decoupled only when the current sheet width compares with λ_{ni} , the effect of recombination on MR then becomes obvious.

ion-inertial length: $d_i \sim n_i^{-0.5}$, Hall effect becomes efficient only when the current sheet width compares with d_i .

Theory and Numerical simulations

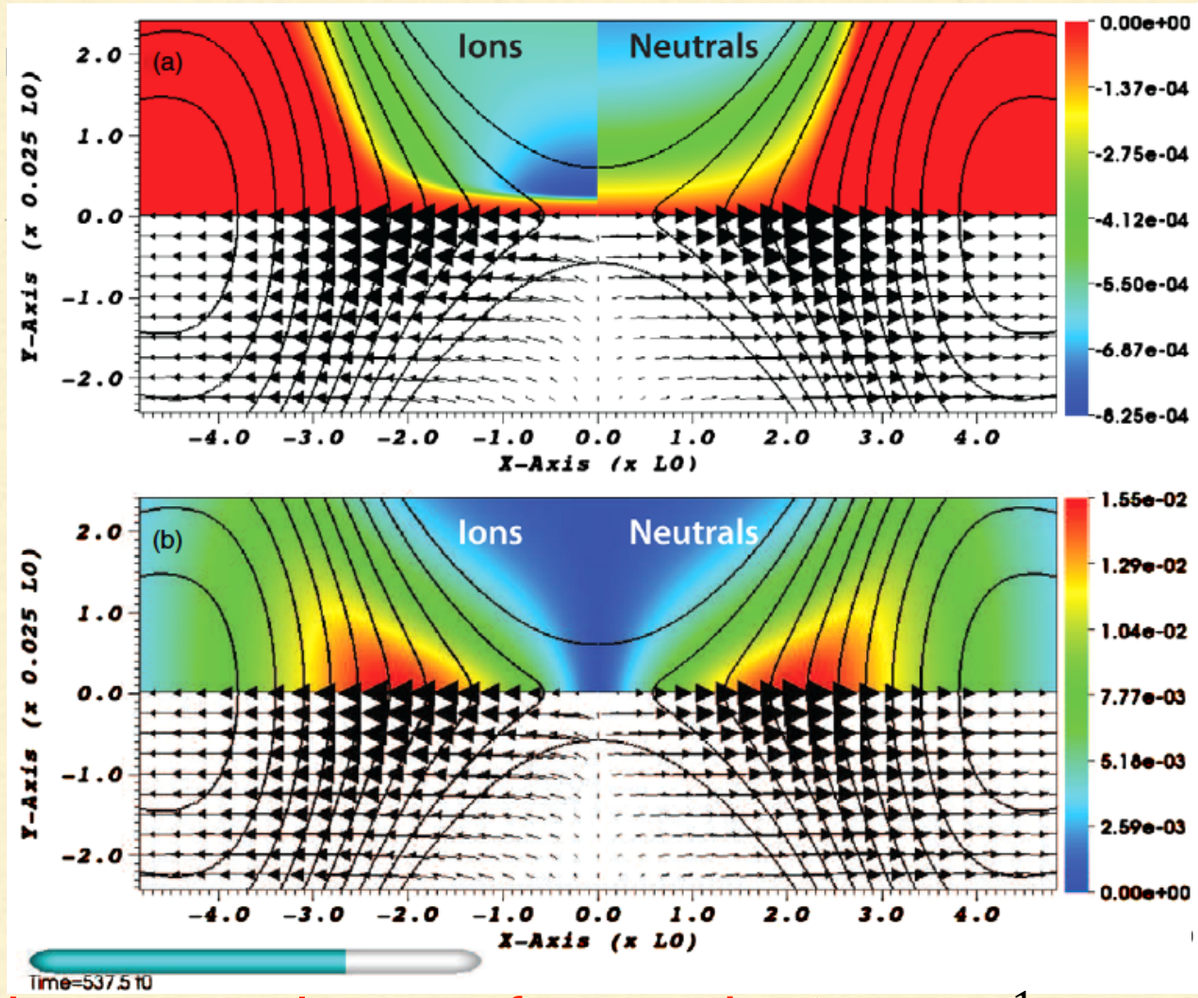

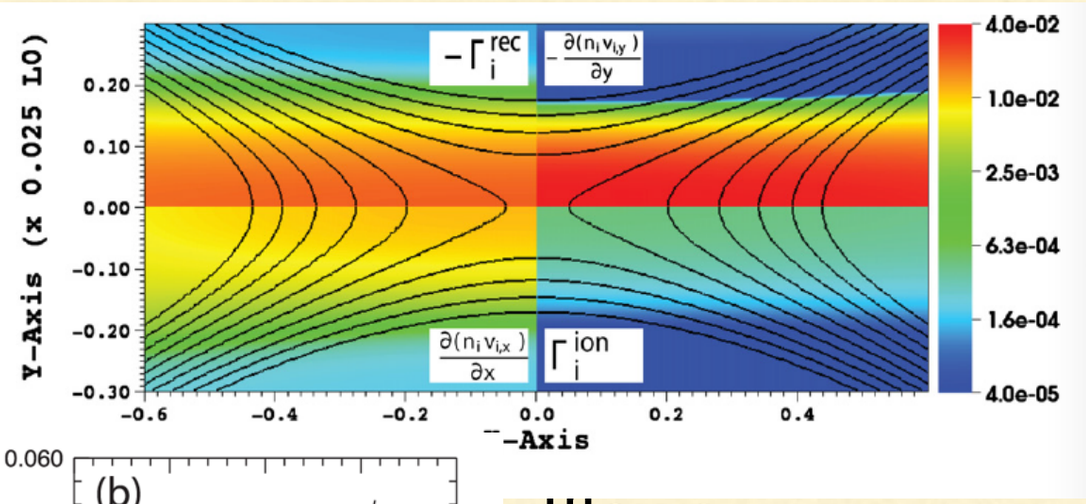

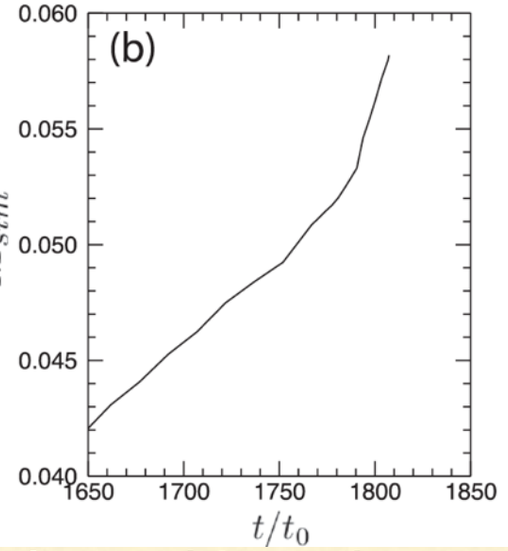

al

uttlows;

combined with

endent of Lundquist

rate by 15%.

ion-neutral mean free path: $\lambda_{ni} \sim n_i^{-1}$, neutrals and ions become decoupled only when the current sheet width compares with λ_{ni} , the effect of recombination on MR then becomes obvious.

ion-inertial length: $d_i \sim n_i^{-0.5}$, Hall effect becomes efficient only when the current sheet width compares with d_i .

Theory and Numerical simulations

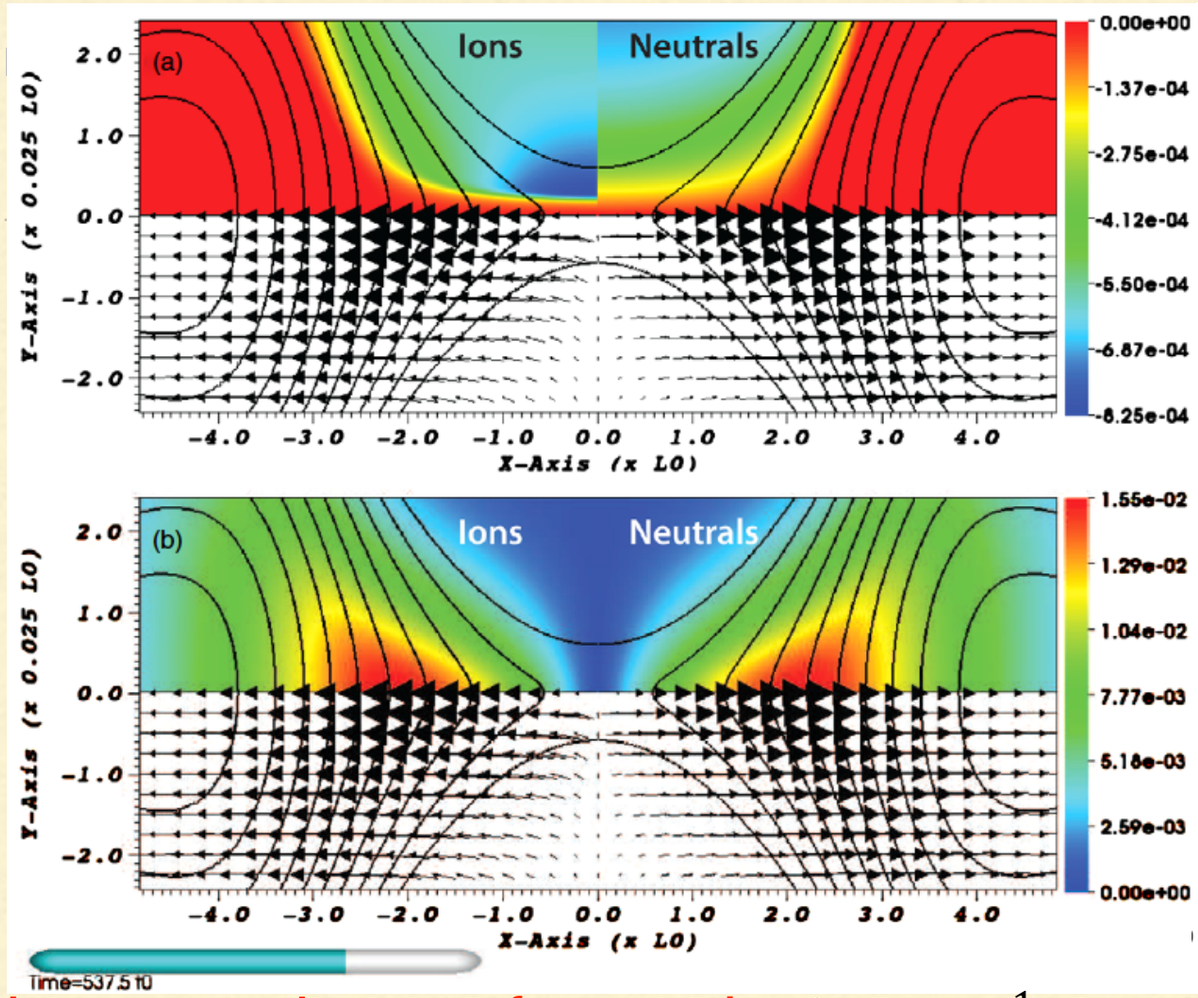

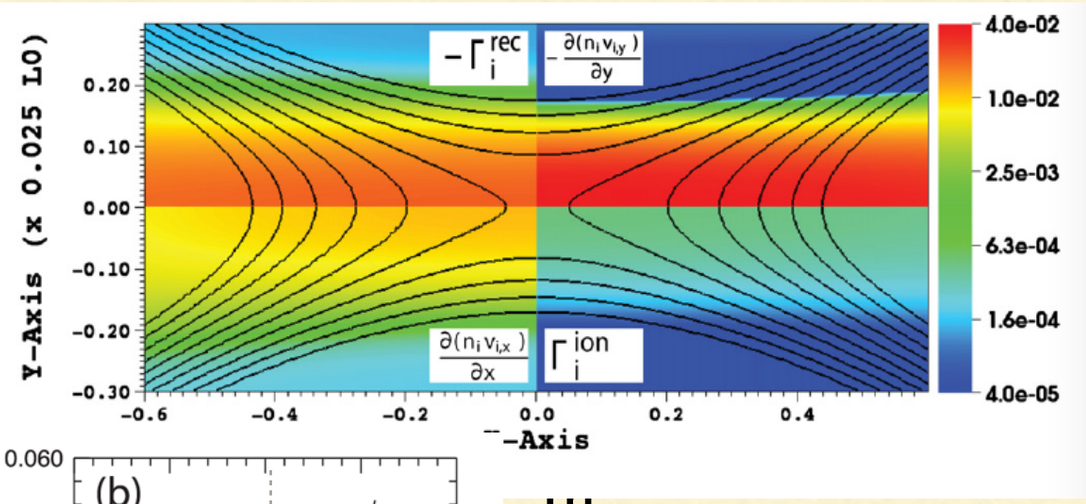

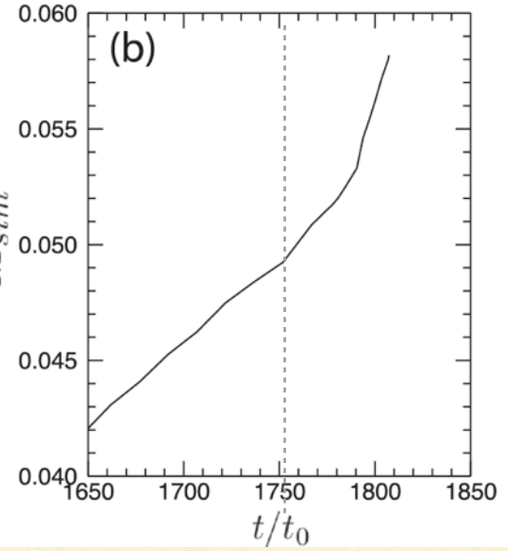

al

utflows;

combined with

endent of Lundquist

rate by 15%.

ion-neutral mean free path: $\lambda_{ni} \sim n_i^{-1}$, neutrals and ions become decoupled only when the current sheet width compares with λ_{ni} , the effect of recombination on MR then becomes obvious.

ion-inertial length: $d_i \sim n_i^{-0.5}$, Hall effect becomes efficient only when the current sheet width compares with d_i .

- **This aim of this work:**

- (1) Study the physical mechanisms about MR around the solar TMR region.

- (2) To figure out how high a temperature the plasma in a reconnection process around the solar TMR can be heated to. Is that possible to produce the Si IV emission lines?

- **Simulations in this work:**

- (1) Both the neutral density and the reconnection magnetic fields are about two orders of magnitude higher than those in the previous work by Leake et al 2012, 2013; Murphy & Lukin 2015; Alvarez Laguna et al 2017

- (2) We use the same Reacting Multi-Fluid plasma-neutral module within the HiFi framework, and the guide field is included.

Numerical Results

- Ni et al 2018, APJ: http://adsabs.harvard.edu/abs/2018ApJ...852...95N
- Ni et al 2018, PoP: http://adsabs.harvard.edu/abs/2018PhPl...25d2903N
- Ni et al 2018, will be submitted

Two different radiative cooling models

(1) A simple radiative cooling model :

$$L_{rad1} = \Gamma_i^{ion} \phi_{eff}$$

where $\phi_{eff} = 33$ eV$= 5.28 \times 10^{-18}$ J. The ionization rate Γ_i^{ion} is defined as

$$\Gamma_i^{ion} = \frac{n_n n_e A}{X + \phi_{\rm ion}/T_e^*} \left(\frac{\phi_{\rm ion}}{T_e^*}\right)^K \exp(-\frac{\phi_{\rm ion}}{T_e^*}),$$

represents the radiative losses that are due to atomic physics such as radiative recombination, the excited states are not tracked.

The radiative cooling is turned off when the plasmas are fully ionized.

(2) A model calculated by using the OPACITY project and CHIANTI databases, more realistic for chromosphere plasmas:

$$L_{rad2} = C_E n_e (n_n + n_i) 8.63 \times 10^{-6} T^{-1/2} \times \sum_{i=1}^{2} E_i \Upsilon_i exp(-eE_i/k_B T)$$

where $C_E = 1.6022 \times 10^{-12}$ erg eV^{-1}, $E_1 = 3.54$ eV and $E_2 = 8.28$ eV, $\Upsilon_1 = 0.15 \times 10^{-3}$ and $\Upsilon_2 = 0.065$. A three level hydrogen atom with two excited levels are included in this function, and E_1 and E_2 are the excited level energies. The unit for the temperature in

In our work, the initial radiative cooling L_{rad2} in (2) is three orders of magnitude higher than L_{rad1} in (1).

(1) using the simple radiative cooling model

$$L_{rad} = \Gamma_i^{ion} \phi_{eff}$$

The Differences in Initial Conditions and Evolution Equations among the Six Simulation Cases

	Case A	Case A0	Case B	Case C	Case D	Case E
b_p	1	1	1	0.2	2	3
with Hall and ν_{en}	No	No	Yes	No	No	No
with non-equilibrium ionization and recombination	Yes	No	Yes	Yes	Yes	Yes

Characteristic values:

$n_\star = 10^{21}\ \mathrm{m}^{-3}$ $B_\star = 0.05\ \mathrm{T}{=}500\ \mathrm{G}.$ $L_\star = 100\ \mathrm{m}.$

Initial conditions:

$n_{n0} = 0.5 n_\star = 0.5 \times 10^{21}\ \mathrm{m}^{-3}$

$f_{i0} = n_{i0}/(n_{i0} + n_{n0}) = 0.01\%.$

$T_{i0} = T_{n0} = 8400\ \mathrm{K}$

$$A_{z0}(y) = -b_p \lambda_\psi \ln\left[\cosh\left(\frac{y}{\lambda_\psi}\right)\right]$$

$$B_{z0}(y) = b_p \Big/ \left[\cosh\left(\frac{y}{\lambda_\psi}\right)\right]$$

Non-equilibrium ionization-recombination effects on MR

With

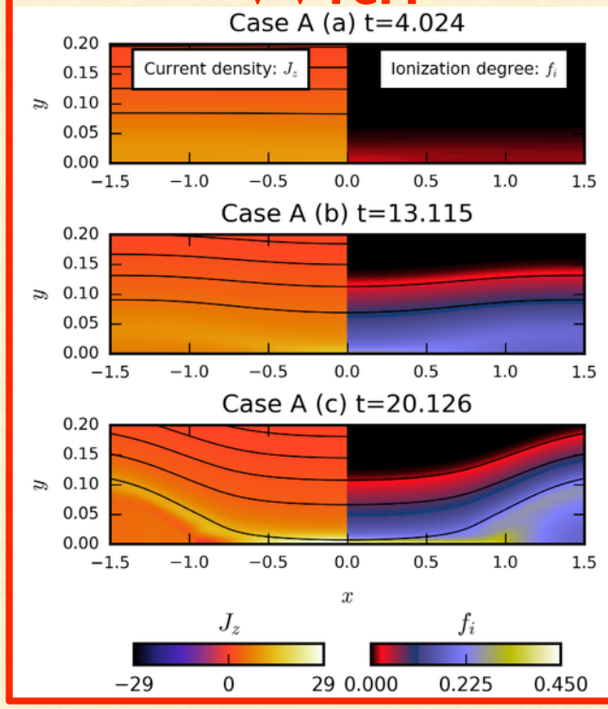

Without

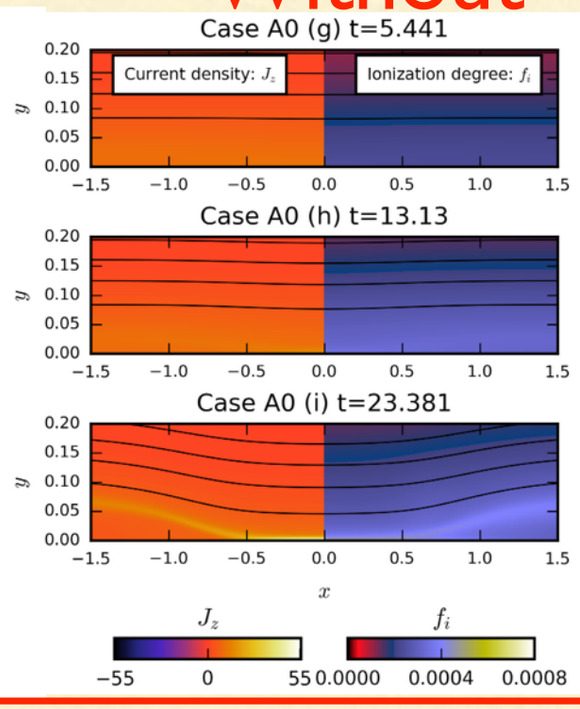

With

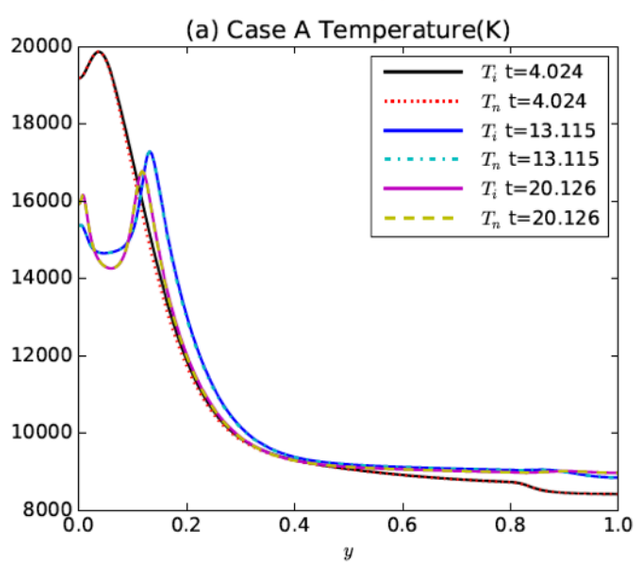

Without

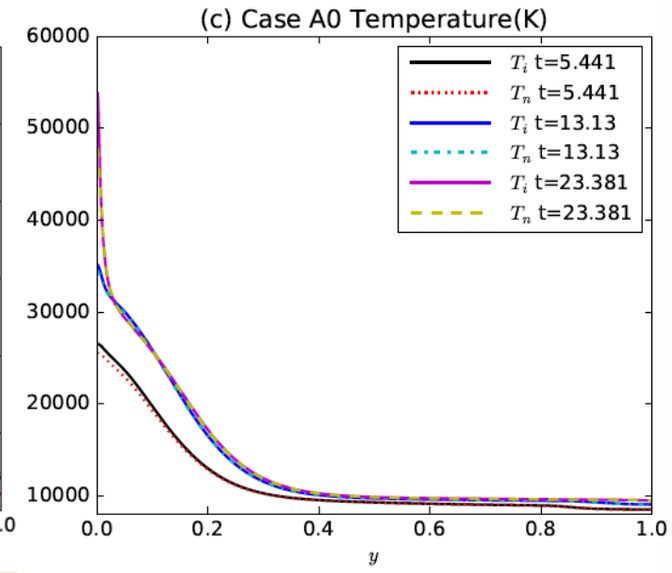

The non-equilibrium ionization-recombination effects make the temperature increases inside the CS more difficult, the strong temperature increases in the previous one-fluid simulations are overestimated.

Effects of beta（magnetic field strength）on MR

500 G

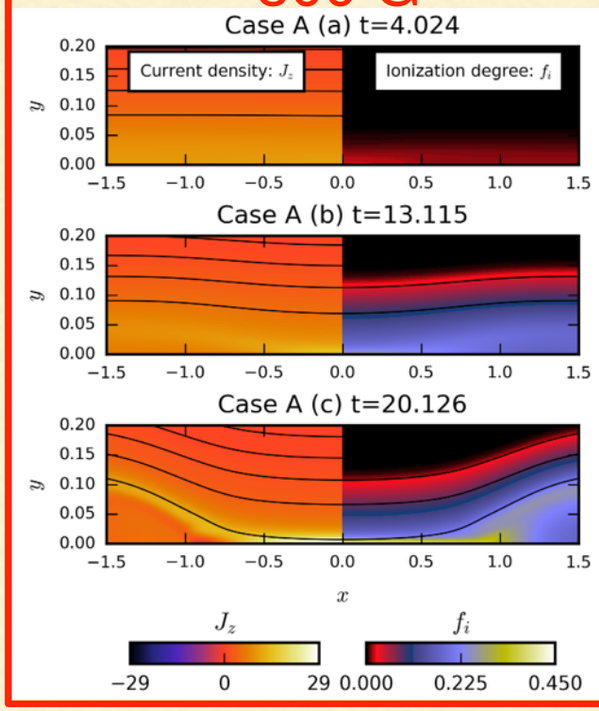

100 G

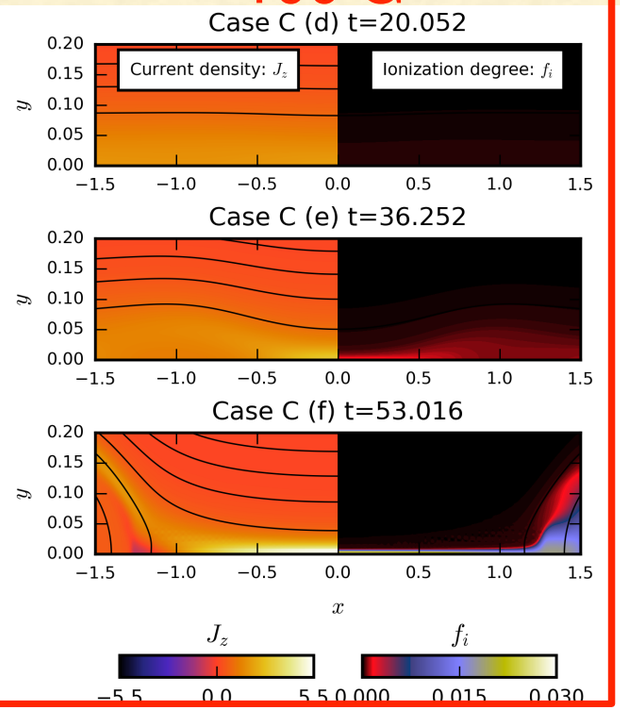

500 G

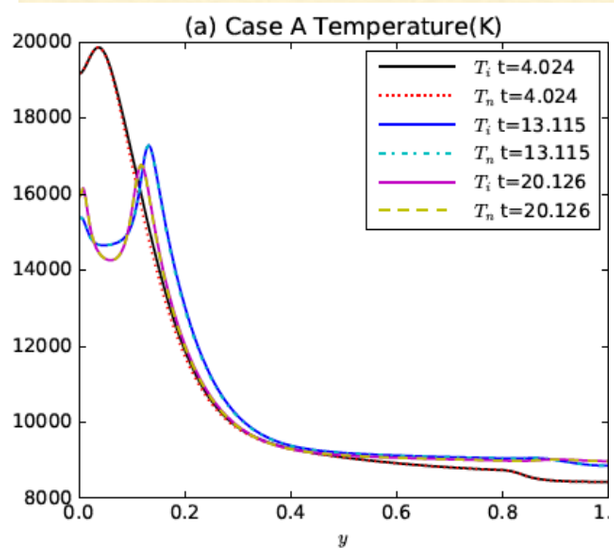

100 G

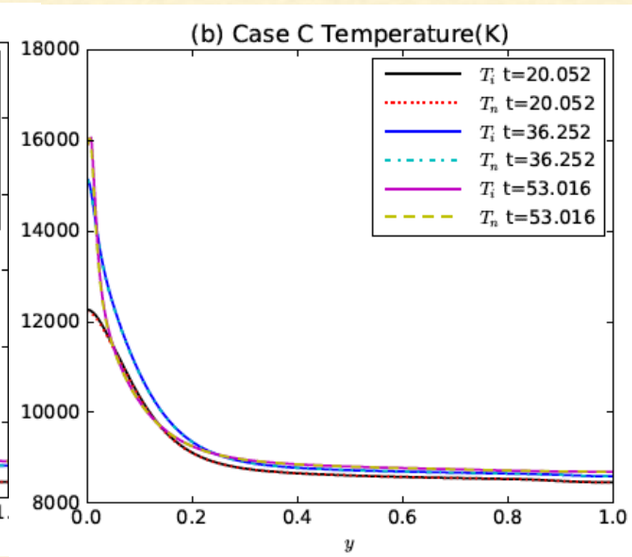

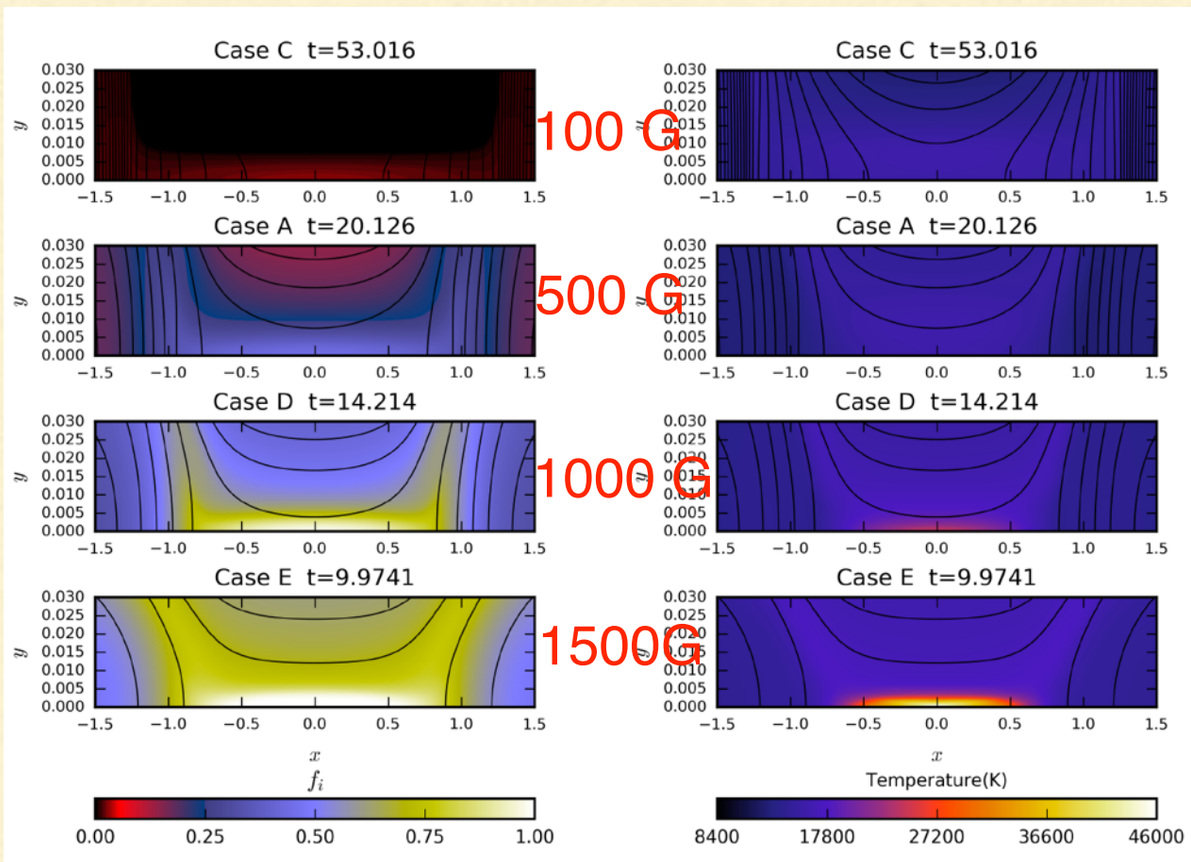

When the magnetic fields in excess of a kilogauss, the initially weakly ionized plasmas become fully ionized inside the CS, the CS is strongly heated above 20,000 K. The maximum one reaches 46,000 K in Case E .

Effects of beta（magnetic field strength）on MR

500 G

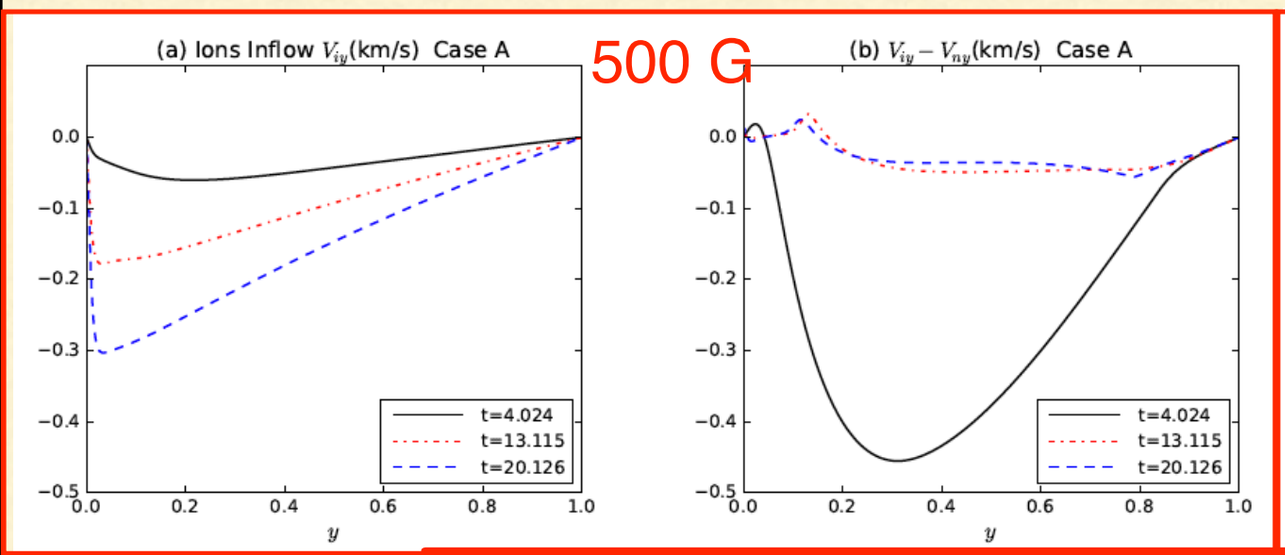

100 G

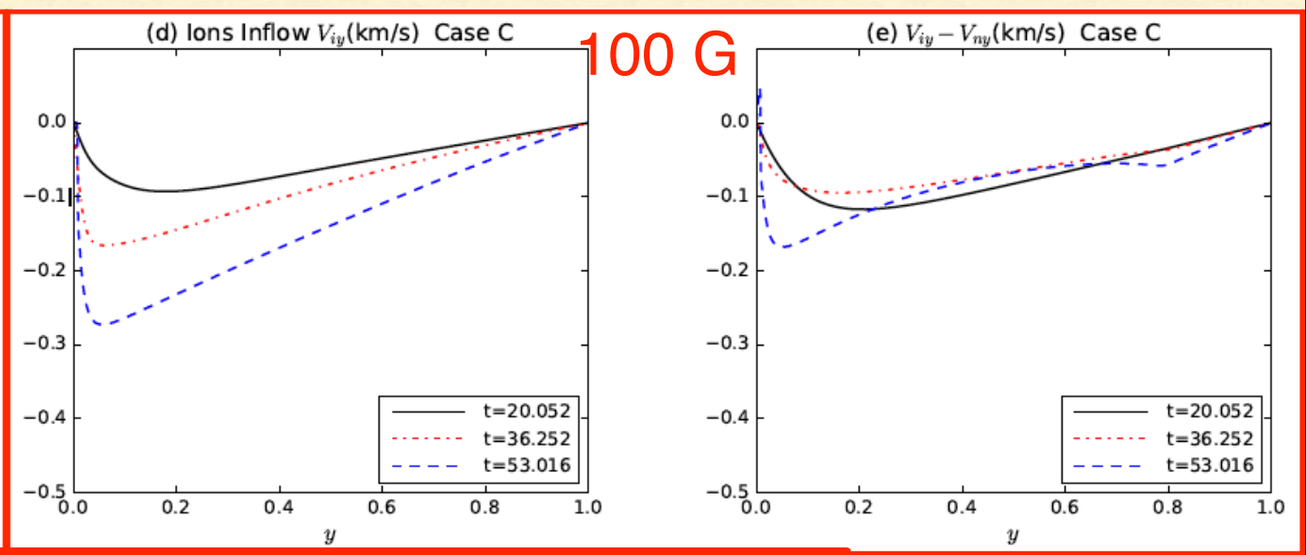

The four terms contribute to $\partial n_i/\partial t$

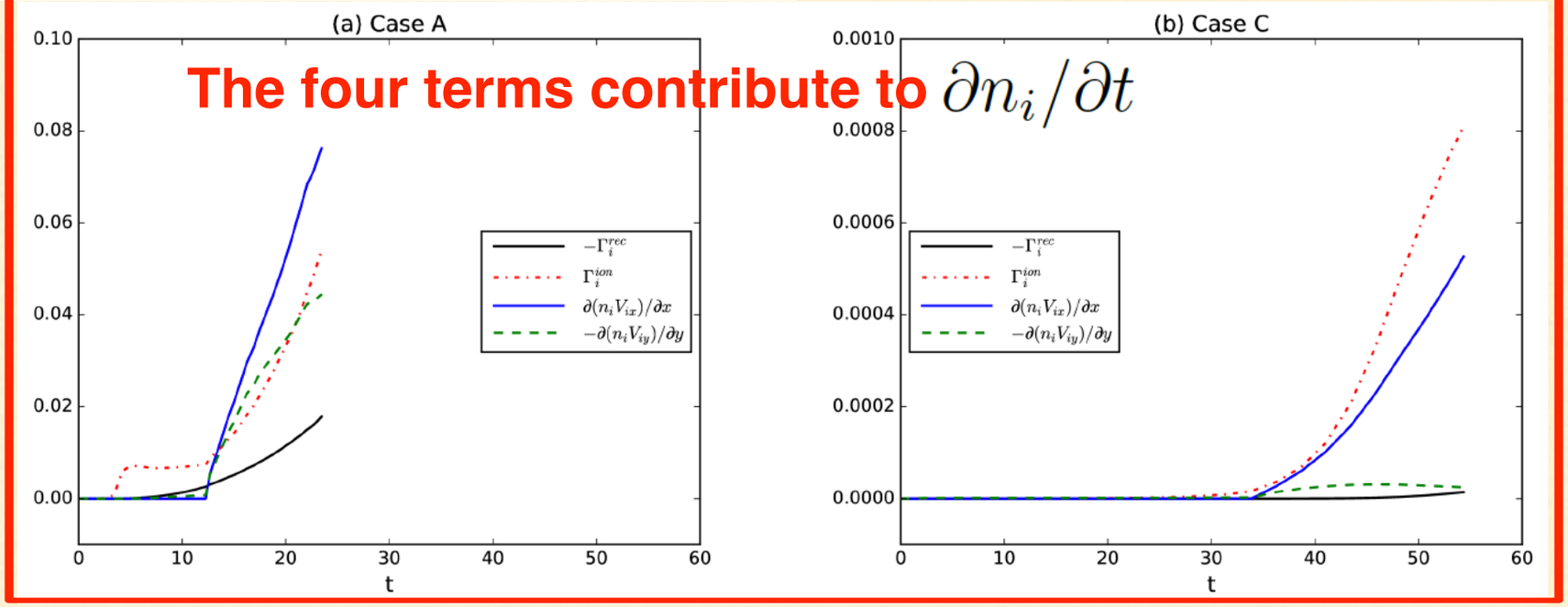

（1） The ionized and neutral fluid flows are **well-coupled throughout the reconnection region** in Case A with low beta, **the decoupling appears** in Case C with **beta=1.46.**

（2） **The ionization rate is always higher than the recombination rate** in all the cases, which is different from the previous high beta weak magnetic field simulations (Leake et al 2012,2013).

Effects of beta（magnetic field strength）on MR

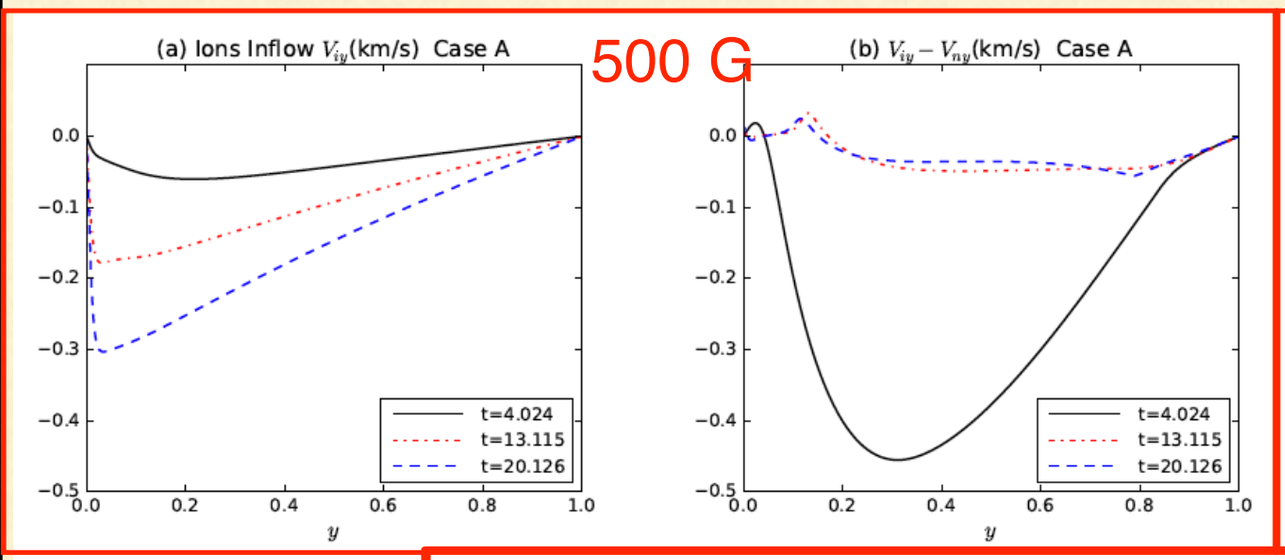

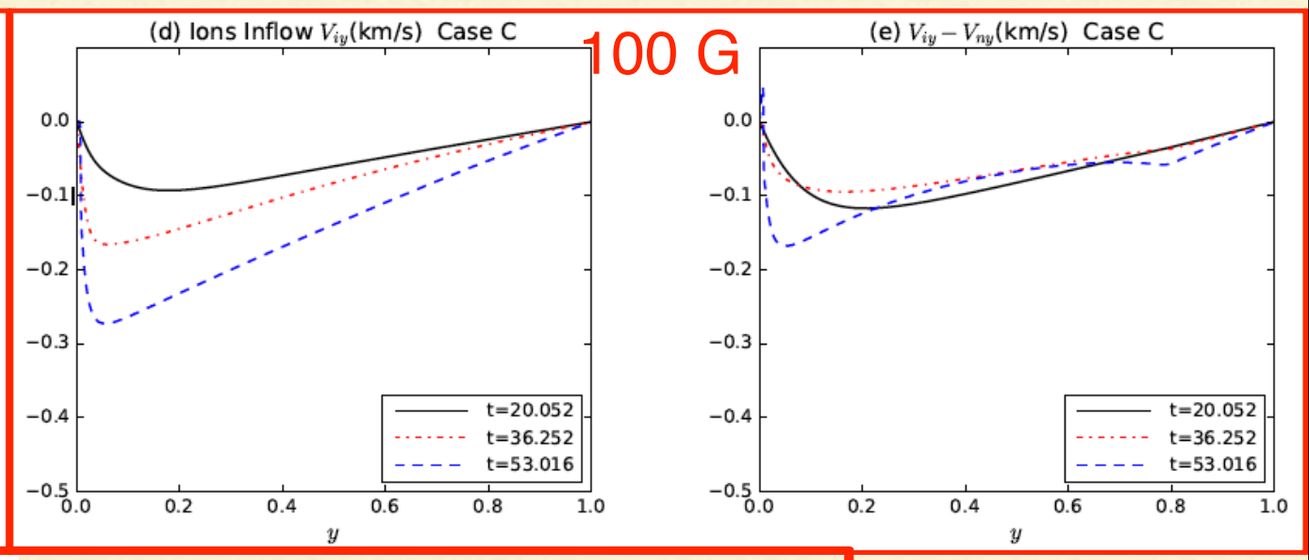

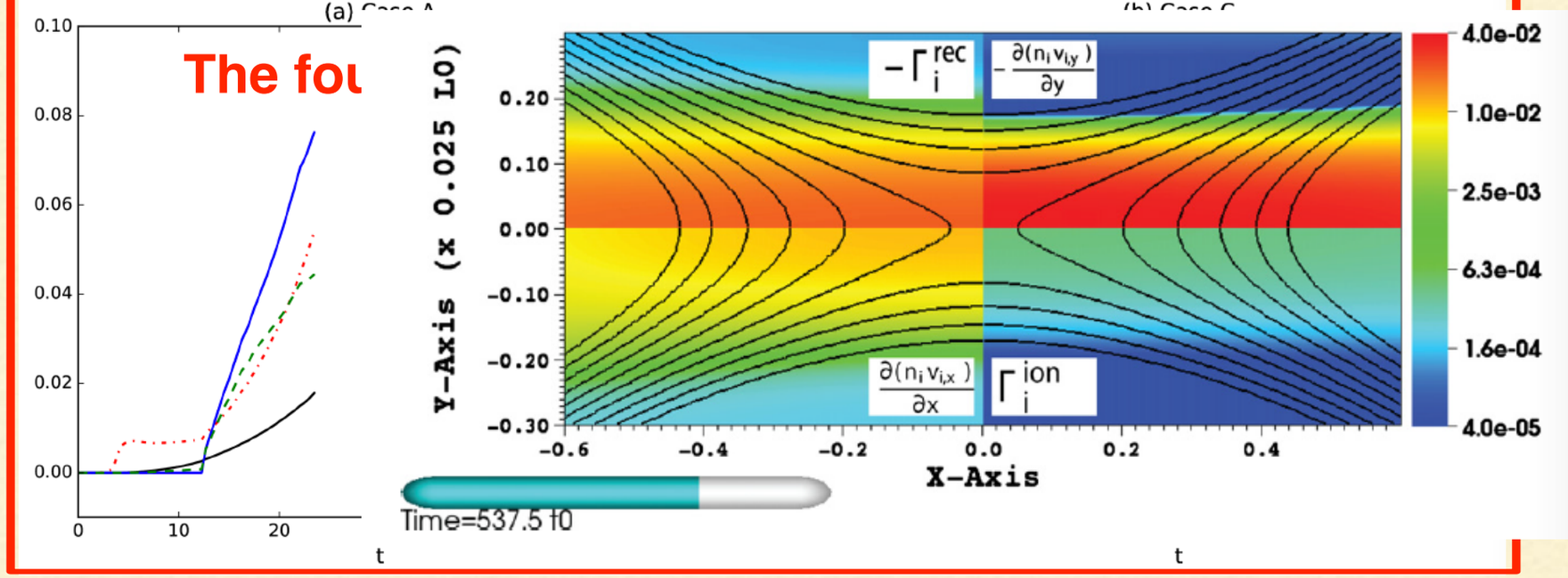

（1） The ionized and neutral fluid flows are well-coupled throughout the reconnection region in Case A with low beta, the decoupling appears in Case C with beta=1.46.

（2） The ionization rate is always higher than the recombination rate in all the cases, which is different from the previous high beta weak magnetic field simulations (Leake et al 2012,2013).

Effects of beta（magnetic field strength）on MR

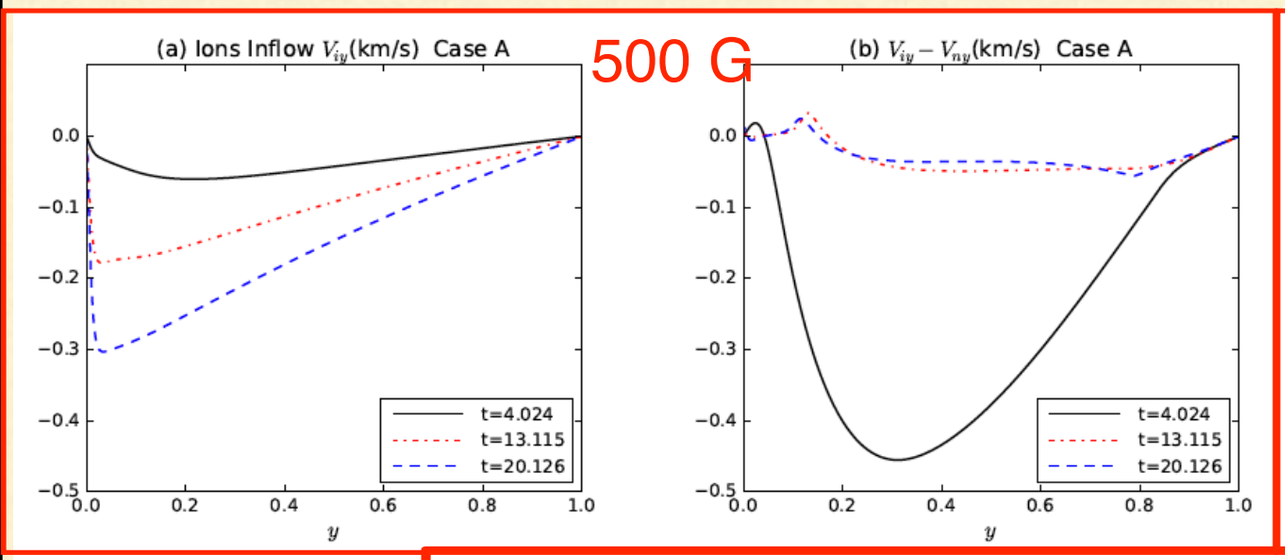

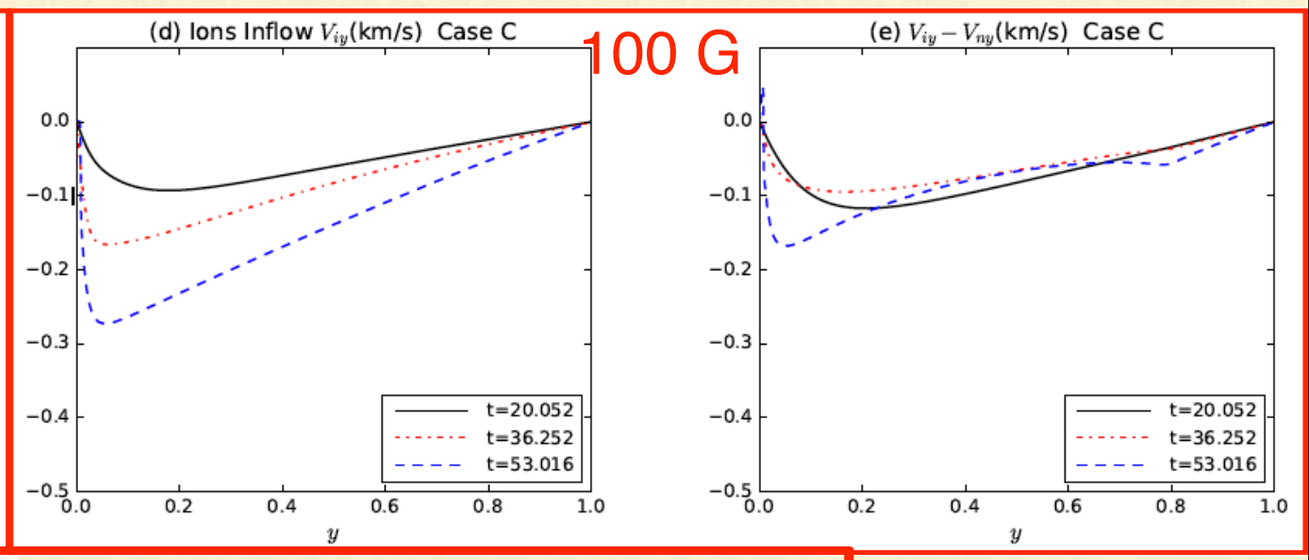

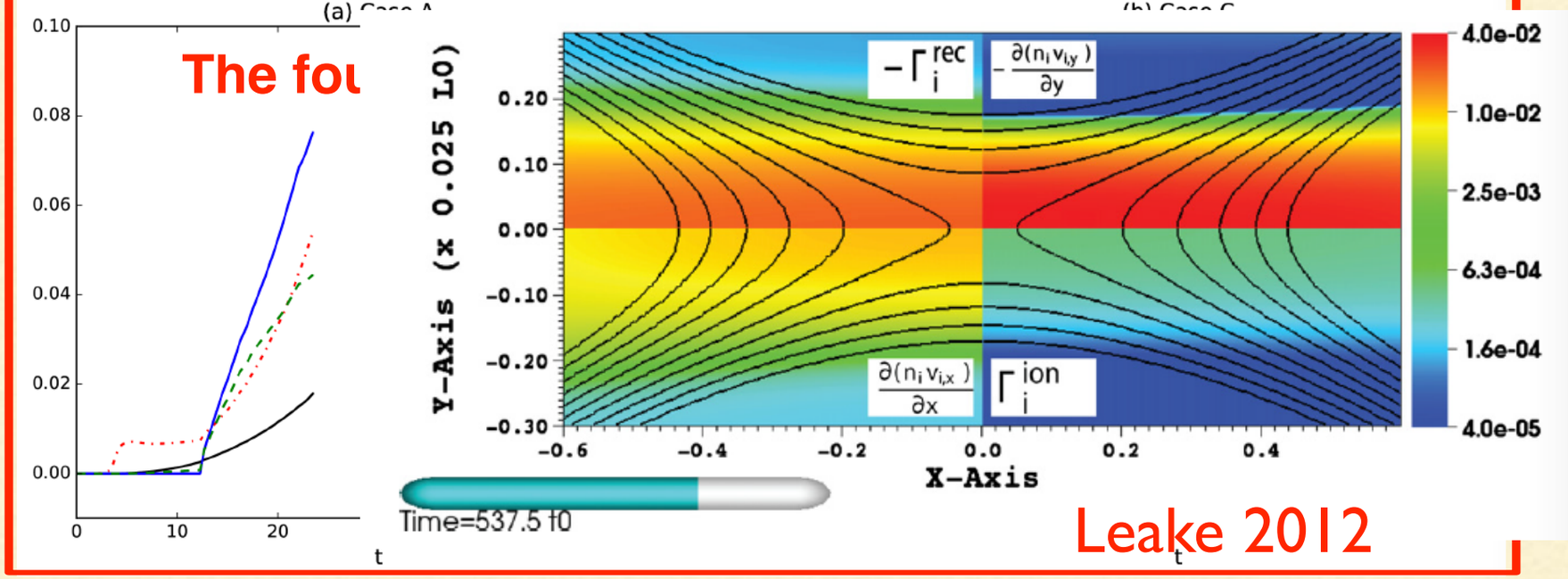

（1） The ionized and neutral fluid flows are **well-coupled throughout the reconnection region** in Case A with low beta, **the decoupling appears** in Case C with **beta=1.46.**

（2） **The ionization rate is always higher than the recombination rate** in all the cases, which is different from the previous high beta weak magnetic field simulations (Leake et al 2012,2013).

Hall effect on MR (compare Case A and B) 500 G

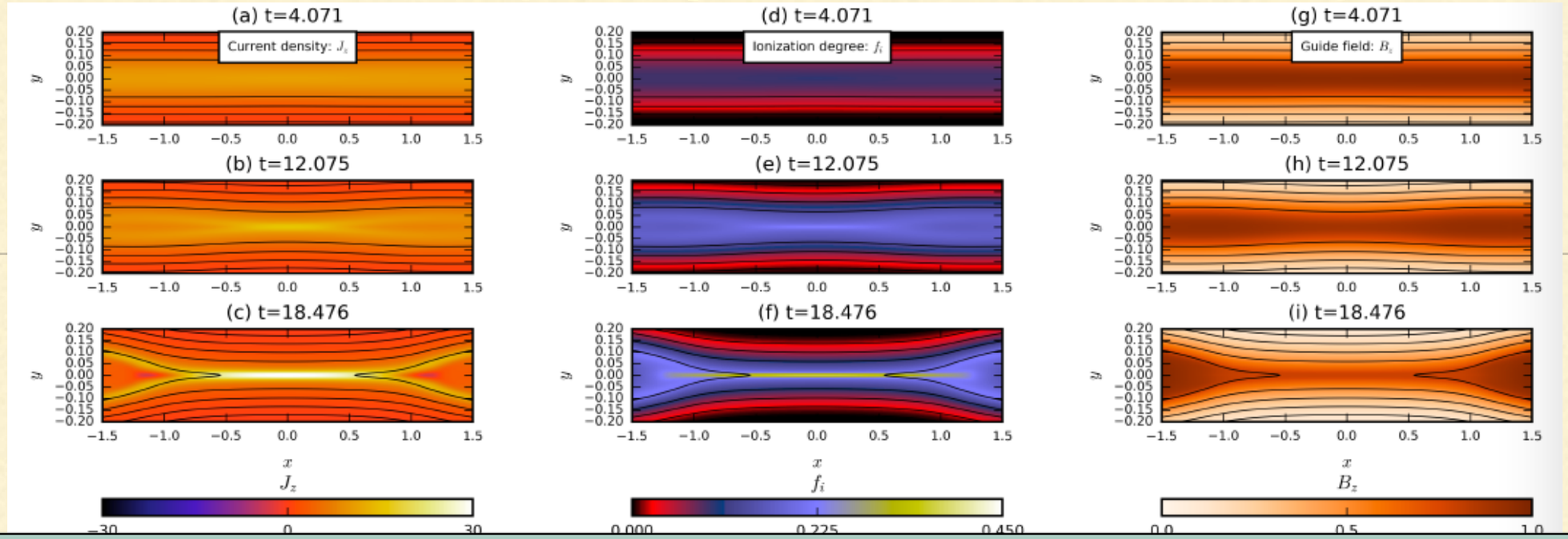

Since di is much smaller than the width of CS, Hall effect does not result in any asymmetries on CS or any significant effects on MR

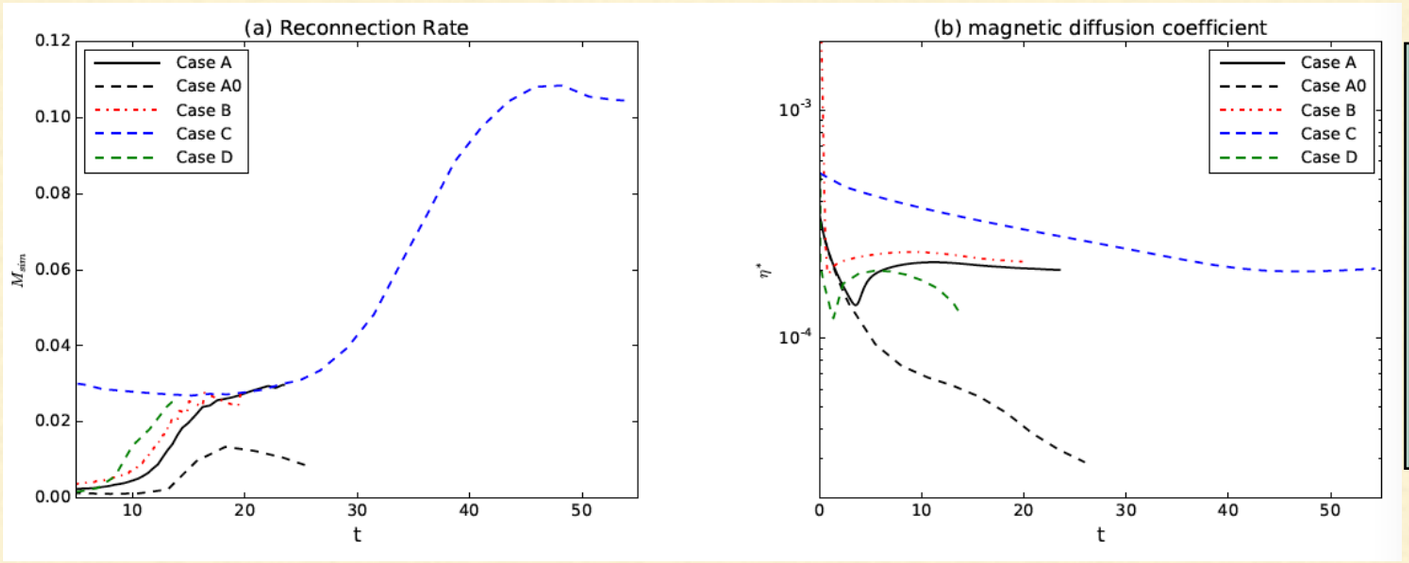

Hall effect only slightly increases the reconnection rate, the collisions between electrons and neutrals become unimportant during the low beta MR process.

(2) using the more realistic radiative cooling model

$$L_{rad2} = C_E n_e (n_n + n_i) 8.63 \times 10^{-6} T^{-1/2} \times \sum_{i=1}^{2} E_i \Upsilon_i exp(-eE_i/k_B T)$$

What one would expect by using this model?

(1) Result in a higher recombination rate than ionization rate?Then result in a faster reconnection as in Alvarez Laguna et al 2017?

(2) Reduce the temperature increases during the MR proses? The high temperature plasmas above 20,000 K might not appear ?

Characteristic values:

$n_\star = 10^{21}\ \mathrm{m}^{-3}$ $B_\star = 0.05$ T=500 G. $L_\star = 100$ m.

Initial conditions:

$n_{n0} = 0.5 n_\star = 0.5 \times 10^{21}\ \mathrm{m}^{-3}$

$f_{i0} = n_{i0}/(n_{i0} + n_{n0}) = 0.01\%$

$T_{i0} = T_{n0} = 8400$ K

$$A_{z0}(y) = -b_p \lambda_\psi \ln\left[\cosh\left(\frac{y}{\lambda_\psi}\right)\right]$$

$$B_{z0}(y) = b_p \Big/ \left[\cosh\left(\frac{y}{\lambda_\psi}\right)\right]$$

Effects of the more realistic radiative cooling model on MR

In Case ALr, CLr and ELr, the more realistic radiative cooling model is applied

		Max (f_i)	Max (T_i)	Max (J_z)	Max $(\lvert V_{iy} - V_{ny} \rvert)$	Max (V_{ix})	Max (M_{sim})	δ_{sim}
500 G	Case ALr	12%	1.95×10^4 K	44	0.185 km/s	21.1 km/s	0.025	0.012
100 G	Case CLr	0.8%	1.6×10^4 K	6	0. 692 km/s	6.3 km/s	0.121	0.017
1500G	Case ELr	72%	2.3×10^4 K	206	0.076 km/s	52.3 km/s	0.016	0.008
500 G	Case A	45%	1.6×10^4 K	29	0.048 km/s	13.9 km/s	0.030	0.015
100 G	Case C	3%	1.6×10^4 K	5.5	0.182 km/s	6.7 km/s	0.109	0.018
1500G	Case E	100%	4.6×10^4 K	192	0.061 km/s	16.4 km/s	0.035	0.003

Quantitatively changes the values of some variables in the MR prcoess. e.g.,for the cases with the same plasma beta, the maximum ionization fractions are lower. The plasmas are not fully ionized even when the reconnection magnetic field is as high as 1500 G, the highest temperature can only reach about 23,000K before this run is killed.

Effects of the more realistic radiative cooling model on MR

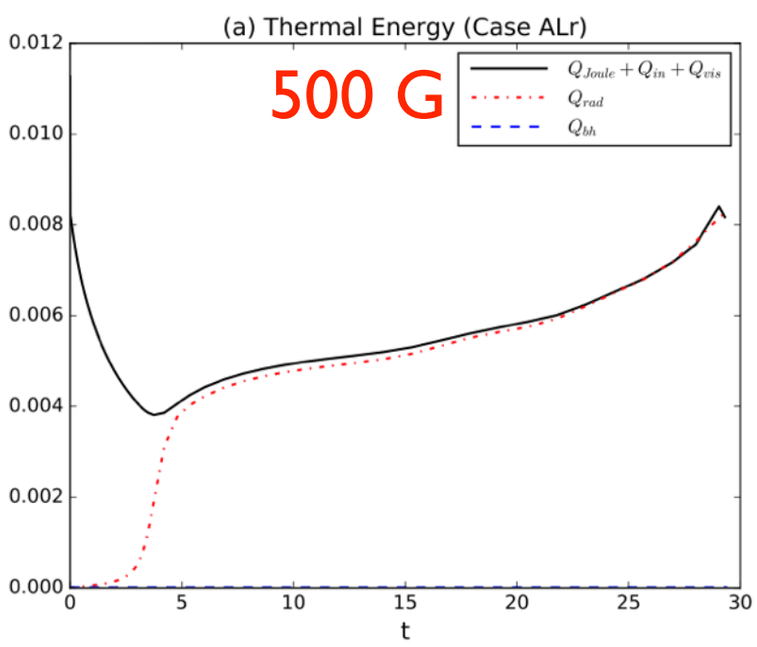

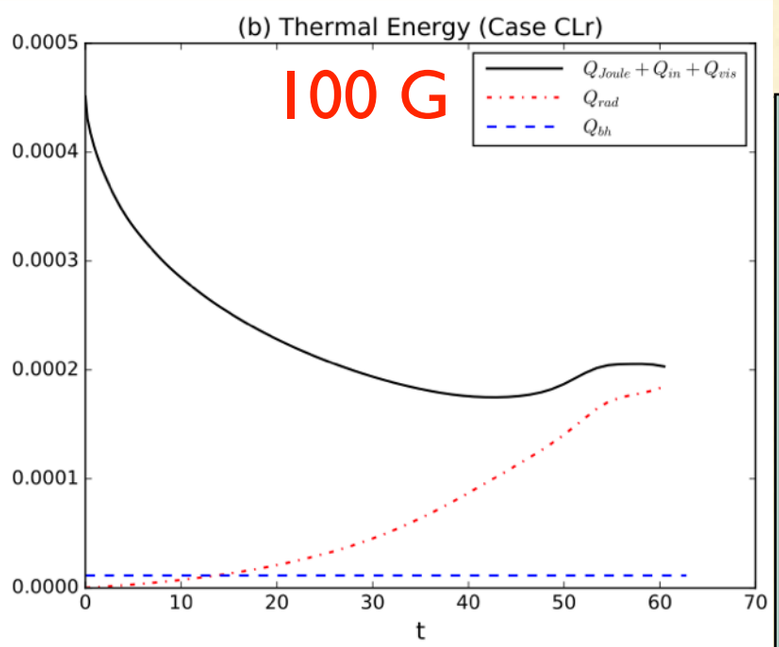

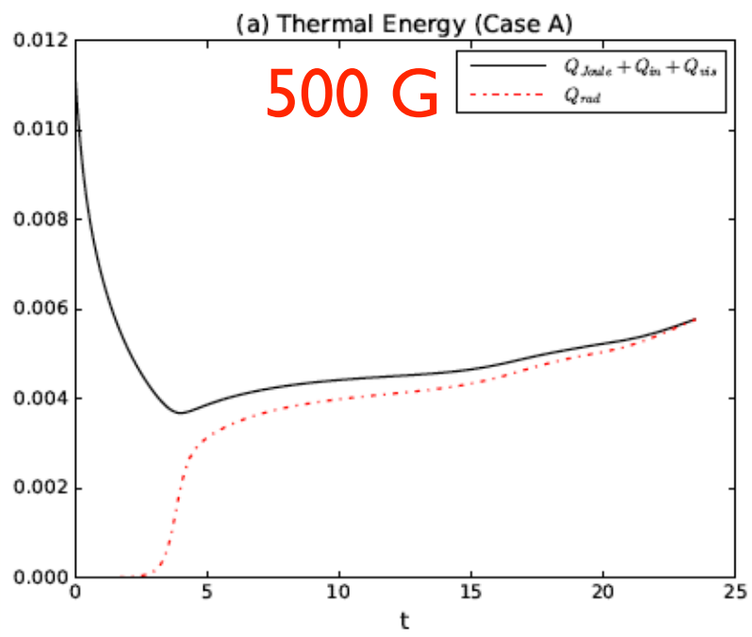

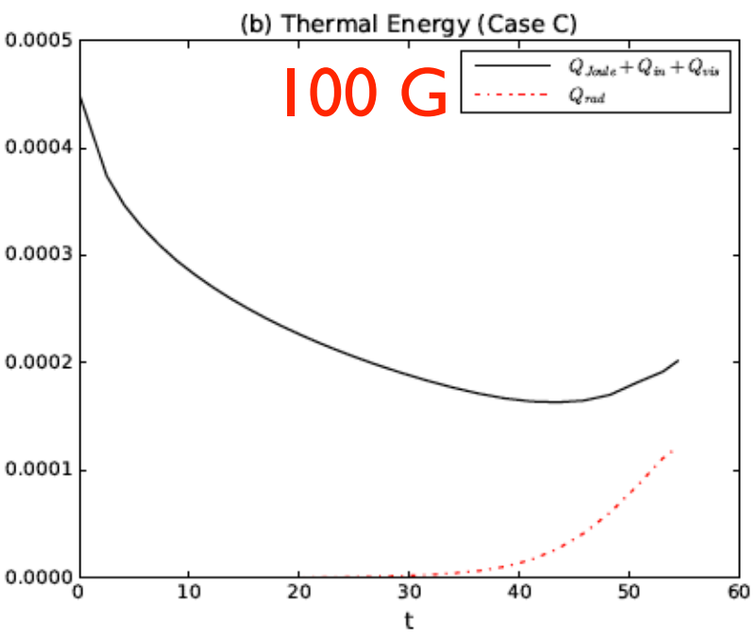

More thermal energy is radiated by using this more realistic model. However, the values of the radiated heat in Case ALr, CLr and ELr are correspondingly at the same order of magnitude as those in Case A, C and E during the MR process before the plasmas are nearly fully ionized.

Effects of the more realistic radiative cooling model on MR

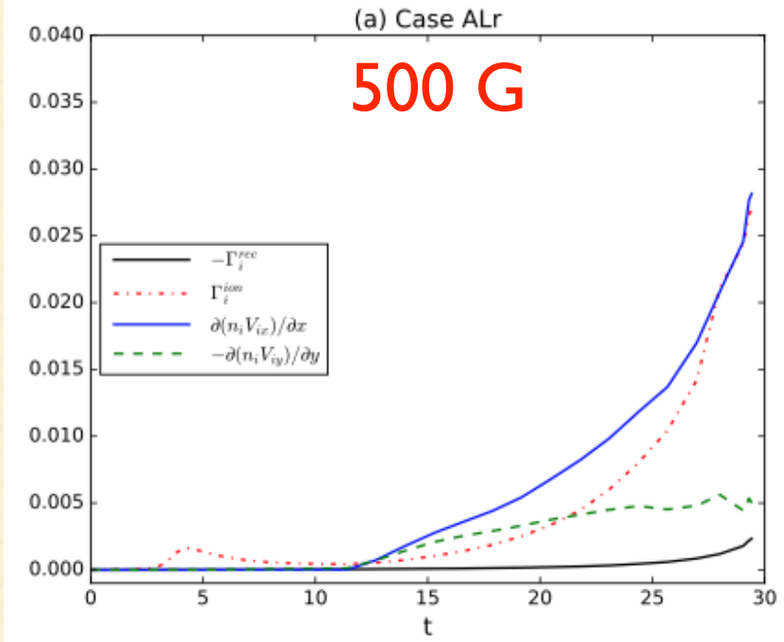

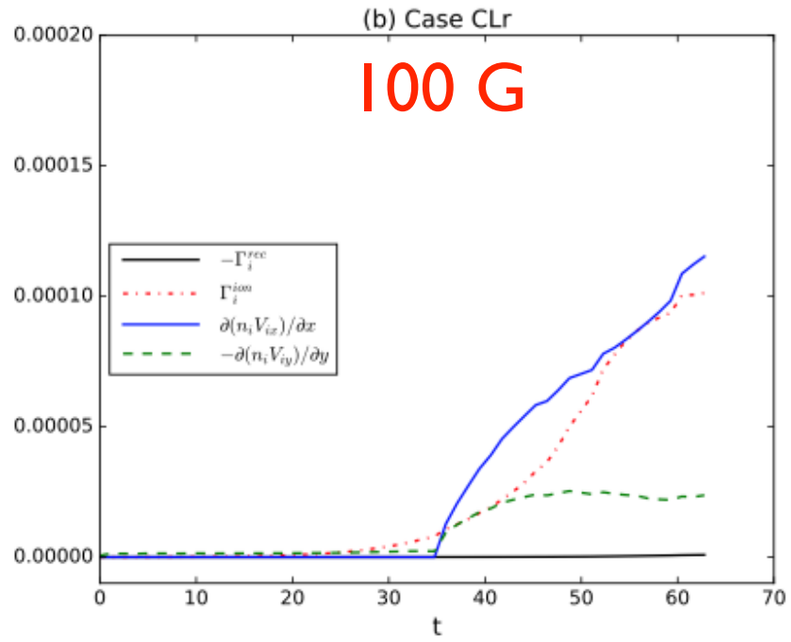

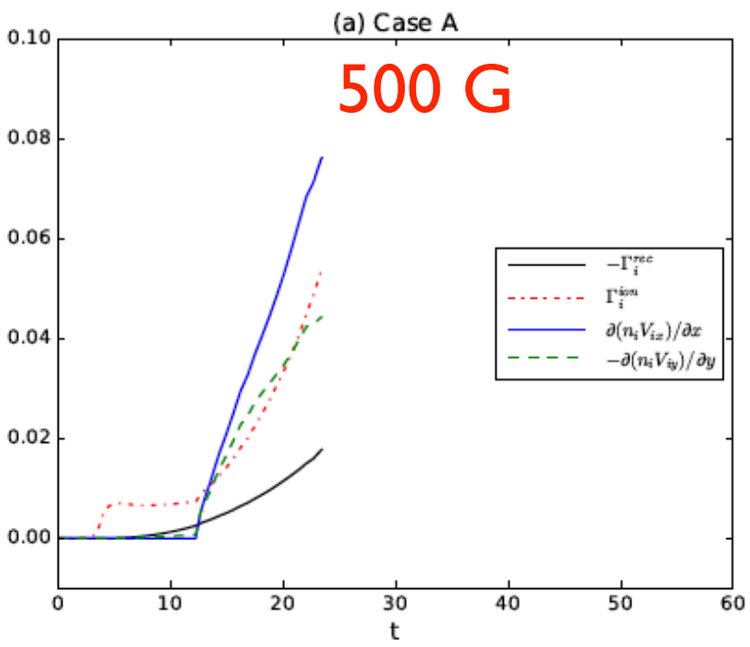

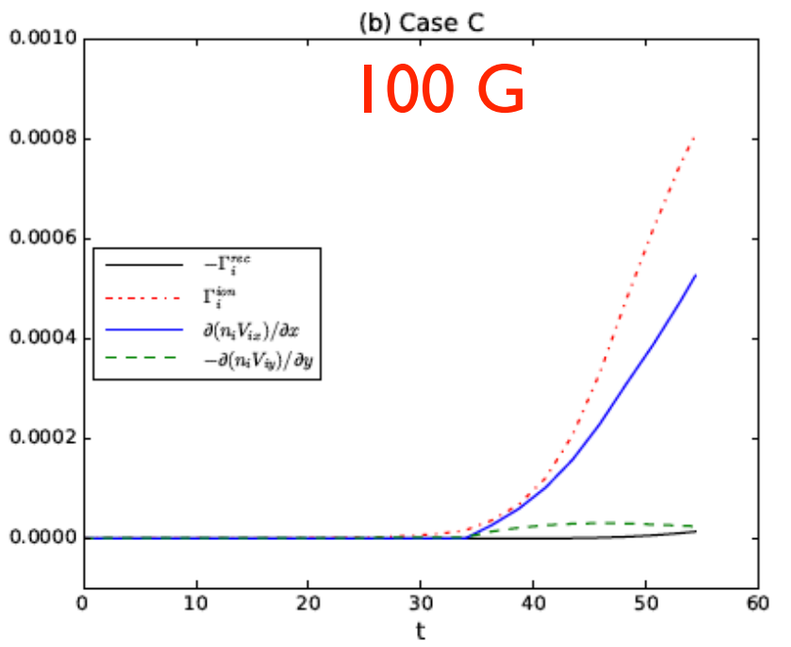

For the cases with the same plasma beta, the four terms contribute to $\partial n_i/\partial t$ are all relatively lower at the same time instant.

However, the ionization rate is still larger than the recombination rate in all the cases under this more realistic cooling model.

Effects of the more realistic radiative cooling model on MR

$$M_{sim} = \eta^* j_{max}/(V_A^* B_{up}) \qquad M_{SP} = 1/\sqrt{S_{sim}} \qquad S_{sim} = V_A^* L_{sim}/\eta^*$$

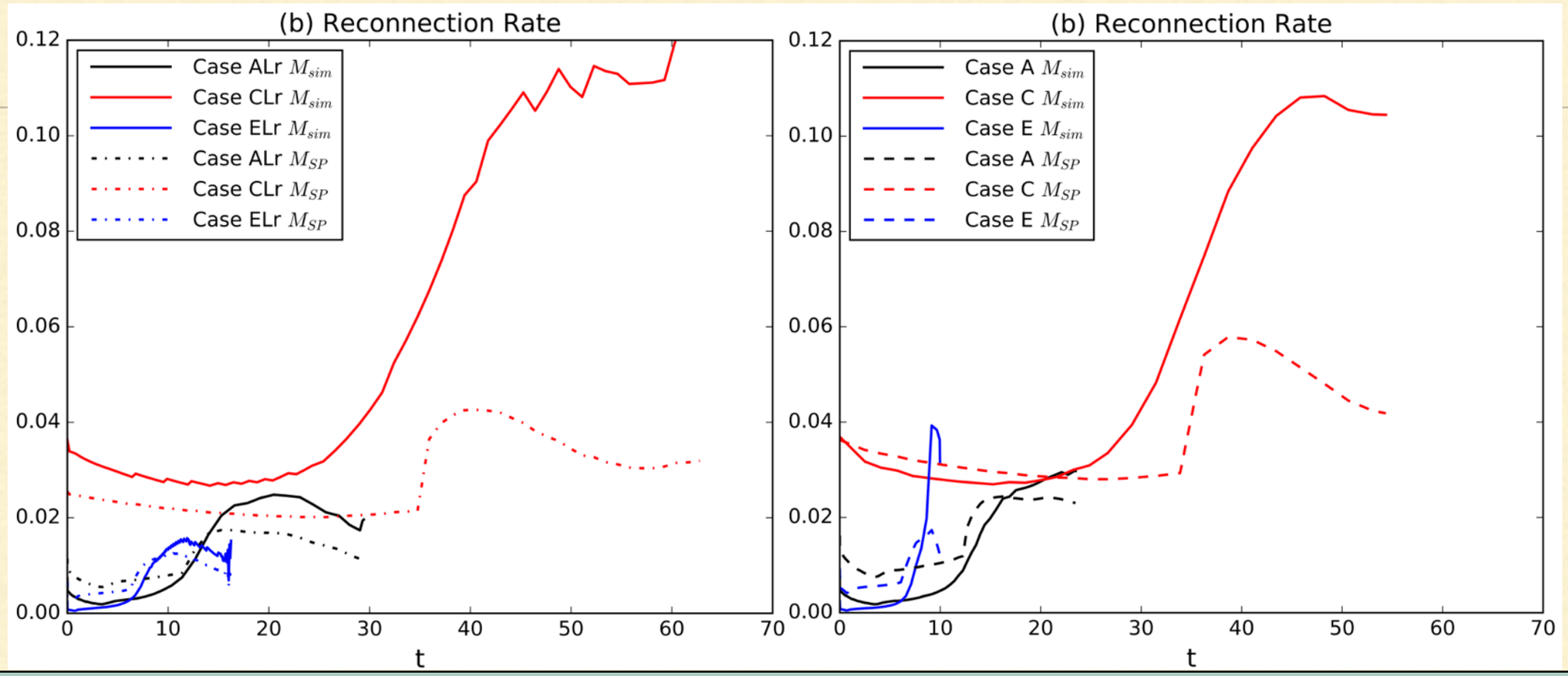

Does not result in qualitatively changes of the characteristics of magnetic reconnection. The decoupling of the ion and neutral inflows is only obvious in Case C and CLr with beta=1.46, which results in a three times faster reconnection rate than that predicted by Sweet-Parker model. The reconnection process more closely resembles the Sweet-Parker model when plasma β is lower.

(3) MR in different length scales (with different Lundquist number)

$n_\star = 10^{21}\ \mathrm{m}^{-3}$ $B_\star = 0.05$ T=500 G. $T_\star = 1.441 \times 10^5$ K

	$L_\star$ (m)	$t_\star$ (s)	n_{n0}	f_{i0}	T_{i0}	b_p	β_0	Radiative cooling
Case A	100	0.0029	$0.5\ n_\star$	10^{-4}	$0.05829T_\star$	1	0.058	L_{rad1}
Case I	200	0.0058	$0.5\ n_\star$	10^{-4}	$0.05829T_\star$	1	0.058	L_{rad1}
Case II	10^3	0.029	$0.5\ n_\star$	10^{-4}	$0.05829T_\star$	1	0.058	L_{rad1}
Case III	10^4	0.29	$0.5\ n_\star$	10^{-4}	$0.05829T_\star$	1	0.058	L_{rad1}

The plasmoid cascading process

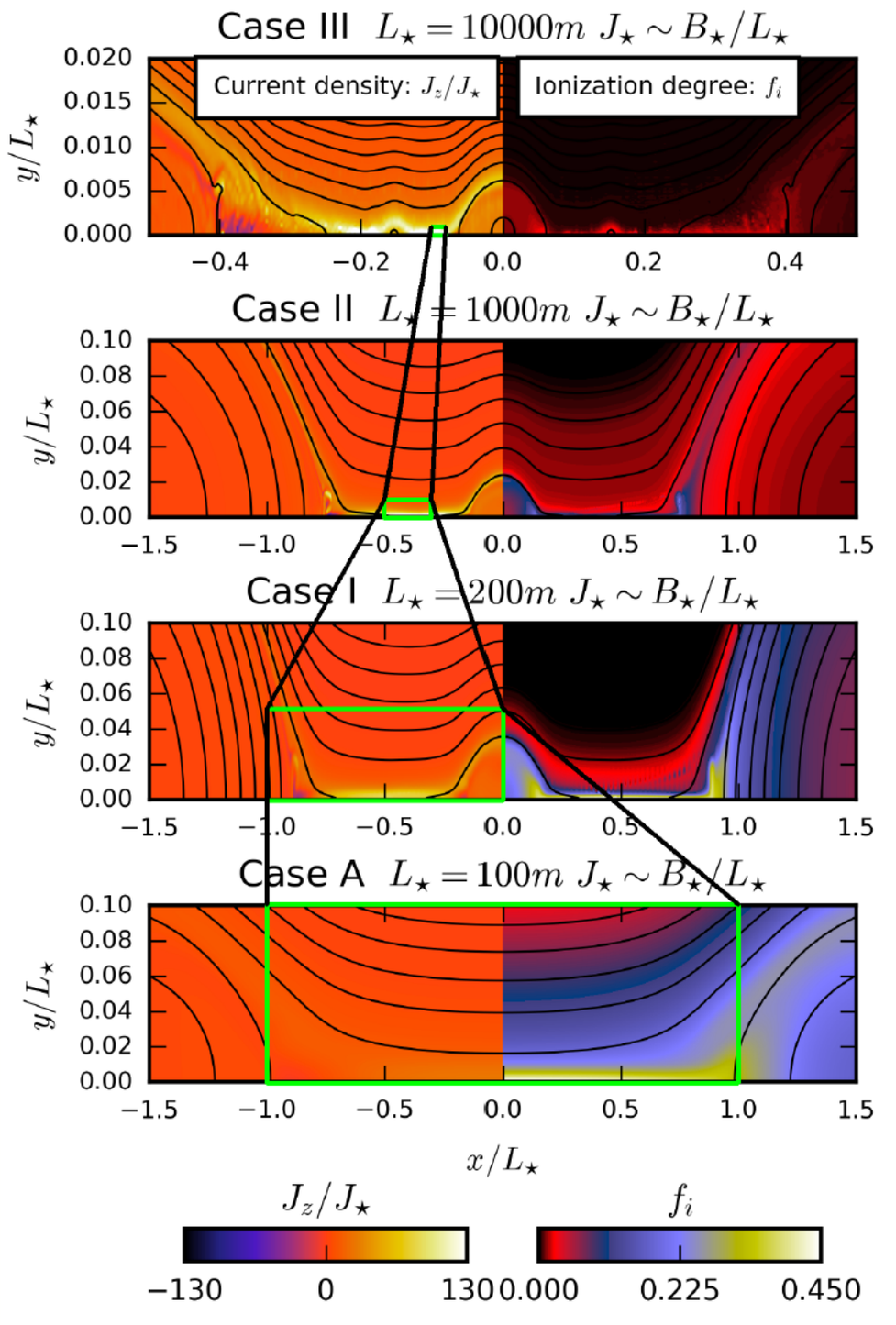

(1) In a MR process with B0=500 G around TMR, the plasmoid cascading terminates in a length scale of 100 m and width of 2 m, which are much larger than both the ion inertial length and ion neutral collision mean free path . Decoupling effects of ions and neutrals and collisionless effects are negligible.

Leake et al 2013

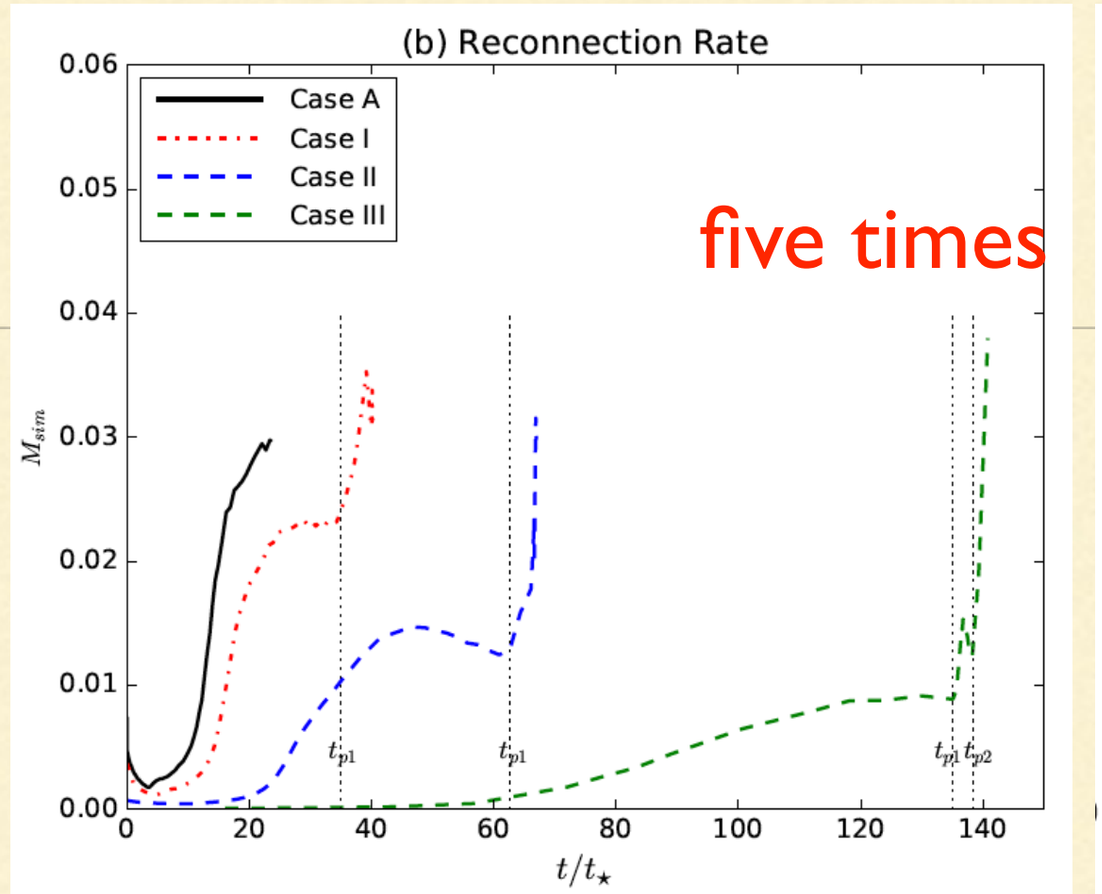

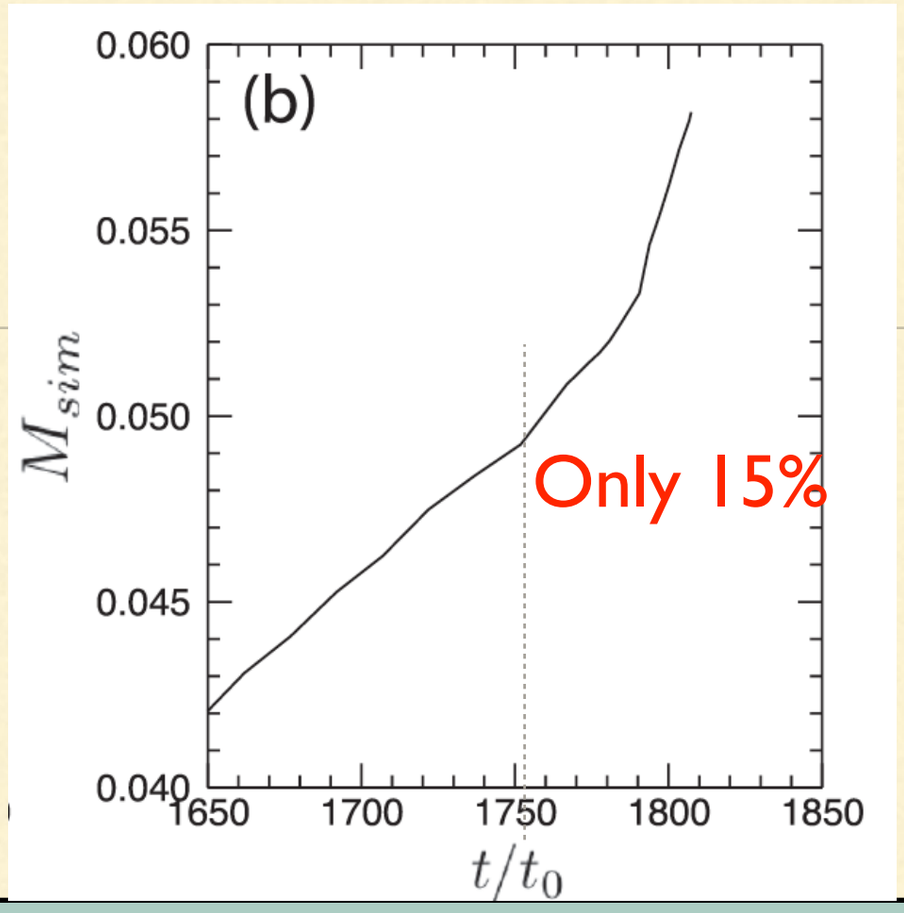

The reconnection rate scales with the Lundquist number as $M_{sim} \sim S_{sim}^{-1/2}$ before plasmoid instabilities appear. After plasmoid instabilities appear, the reconnection rate sharply increases to a high value (about 0.035), which is independent of the Lundquist number. These characteristics are very similar to MR in fully ionized plasmas, but very different from those in the previous low beta studies (Leake et al 2012, 2013).

(4) Magnetic reconnection at different heights in the low Solar atmosphere

$n_\star = 10^{21}\ \mathrm{m}^{-3}$ $B_\star = 0.05$ T=500 G. $T_\star = 1.441 \times 10^5$ K

	$L_\star$ (m)	$t_\star$ (s)	n_{n0}	f_{i0}	T_{i0}	b_p	β_0	Radiative cooling
600 km Case I	200	0.0058	$0.5\ n_\star$	10^{-4}	$0.05829T_\star$	1	0.058	L_{rad1}
300 km Case IV	200	0.0058	$12.5\ n_\star$	10^{-4}	$0.05829T_\star$	5	0.058	L_{rad1}
800 km Case V	200	0.0058	$0.1\ n_\star$	10^{-3}	$0.06559T_\star$	1	0.01305	L_{rad2}

$n_{n0}=0.5n_*$, $b_p=1$ 600 km

$n_{n0}=12.5n_*$, $b_p=5$ 300 km

$n_{n0}=0.1n_*$, $b_p=1$ 800 km

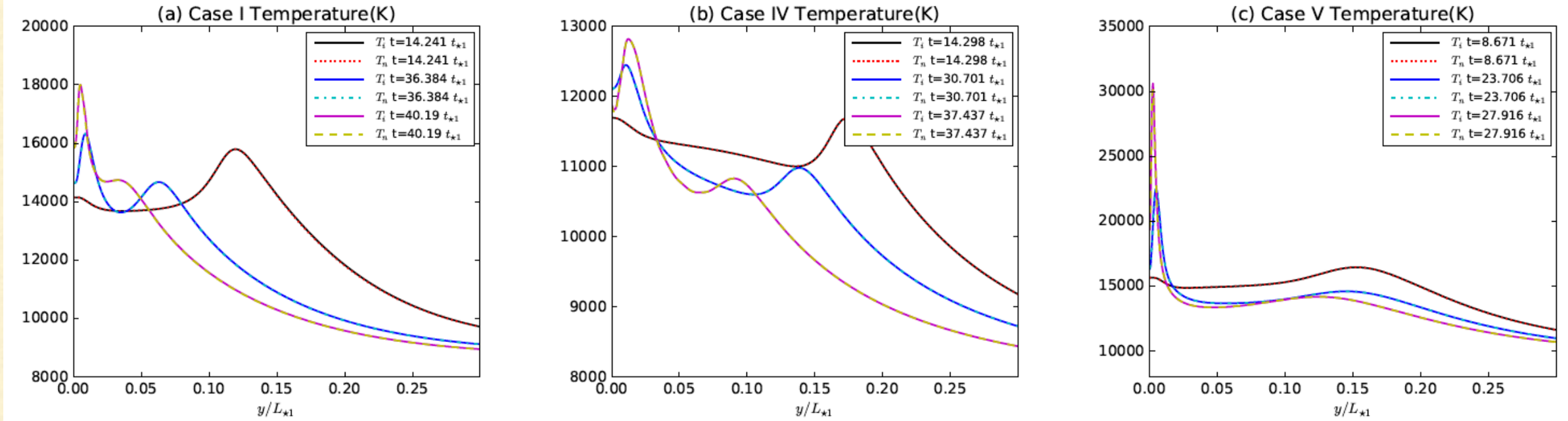

The lower density plasmas at 800 km above the solar surface can be heated above 30, 000 K when the reconnection magnetic field is as high as 500 G. It is more difficult to heat and ionize the high density plasma in the photosphere.

Summary and Conclusions

- （1） Including the non-equilibrium ionization-recombination makes the plasmas heating in a MR process around the TMR more difficult, the high temperature increases in the previous on-fluid MR simulations are probably overestimated. However, when the MR magnetic field is strongly enough, the plasmas can still be heated above 20, 000 K by including the non-equilibrium ionization-recombination and a more realistic radiative cooling model.

- （2） In a MR process with strong magnetic fields and low plasma beta around the solar TMR, the ionization rate is always larger than the recombination rate and the ionized and neutral fluid flows are well-coupled throughout the reconnection region. Plasmoid instability is still the main mechanism to result in fast magnetic reconnection. Plasmoid cascading terminates in a scale which is much larger than both the neutral ion mean free path and ion inertial length. Decoupling effects of ions and neutrals and collisionless effects are negligible.

Future Plans

- (1) Solve the negative density problem
- (2) Include the excited state in the code for the hydrogen gas
- (3) More realistic radiative cooling, solving the radiative transfer equations?
- (4) Larger scale simulations to compare with observations

Reacting Multi-Fluid Model in HiFi

Ionization, Recombination and Charge exchange

The ionization and recombination rates are given by

$$\Gamma_n^{\text{ion}} \equiv -n_n \nu^{\text{ion}},$$

$$\Gamma_i^{\text{rec}} \equiv -n_i \nu^{\text{rec}},$$

with $\Gamma_i^{\text{ion}} = -\Gamma_n^{\text{ion}}$ and $\Gamma_i^{\text{rec}} = -\Gamma_n^{\text{rec}}$. The ionization frequency

$$\nu^{\text{ion}} = \frac{n_e A}{X + \phi_{\text{ion}}/T_e^*} \left(\frac{\phi_{\text{ion}}}{T_e^*}\right)^K \exp(-\frac{\phi_{\text{ion}}}{T_e^*}) \quad \text{m}^3\,\text{s}^{-1}$$

$$\nu^{\text{rec}} = 2.6 \times 10^{-19} \frac{n_e}{\sqrt{T_e^*}} \quad \text{m}^3\,\text{s}^{-1}.$$

The CX reaction rate, $\Gamma^{\text{cx}}$is defined as

$$\Gamma^{\text{cx}} \equiv \sigma_{\text{cx}}(V_{\text{cx}}) n_i n_n V_{\text{cx}},$$

where

$$V_{\text{cx}} \equiv \sqrt{\frac{4}{\pi} V_{Ti}^2 + \frac{4}{\pi} V_{Tn}^2 + V_{in}^2}$$

Reacting Multi-Fluid Model in HiFi

Continuity:

Due to charge neutrality, only the ion and neutral continuity equations are required.

$$\frac{\partial n_i}{\partial t} + \nabla \cdot (n_i \mathbf{v}_i) = \Gamma_i^{ion} + \Gamma_i^{rec}, \qquad \textit{ionization}$$

$$\frac{\partial n_n}{\partial t} + \nabla \cdot (n_n \mathbf{v}_n) = \Gamma_n^{rec} + \Gamma_n^{ion}. \qquad \textit{\& recombination}$$

Momentum:

The electron and ion momentum equations are summed and terms of order $(m_e/m_p)^{1/2}$ and higher are neglected to give:

$$\frac{\partial}{\partial t}(m_i n_i \mathbf{v}_i) + \nabla \cdot (m_i n_i \mathbf{v}_i \mathbf{v}_i + \mathbb{P}_i + \mathbb{P}_e) = \mathbf{j} \times \mathbf{B} + \mathbf{R}_i^{in} + \Gamma_i^{ion} m_i \mathbf{v}_n - \Gamma_n^{rec} m_i \mathbf{v}_i + \Gamma^{cx} m_i (\mathbf{v}_n - \mathbf{v}_i) + \mathbf{R}_{in}^{cx} - \mathbf{R}_{ni}^{cx}.$$

charge-exchange

The neutral momentum equation is

$$\frac{\partial}{\partial t}(m_i n_n \mathbf{v}_n) + \nabla \cdot (m_i n_n \mathbf{v}_n \mathbf{v}_n + \mathbb{P}_n) = -\mathbf{R}_i^{in} + \Gamma_n^{rec} m_i \mathbf{v}_i - \Gamma_i^{ion} m_i \mathbf{v}_n + \Gamma^{cx} m_i (\mathbf{v}_i - \mathbf{v}_n) - \mathbf{R}_{in}^{cx} + \mathbf{R}_{ni}^{cx}.$$

Reacting Multi-Fluid Model in HiFi

Internal Energy:

Again, combining the electron and ion energy equations together and neglecting terms of the order $(m_e/m_p)^{1/2}$ and higher gives:

$$\frac{\partial}{\partial t}\left(\varepsilon_i + \frac{P_e}{\gamma-1}\right) + \nabla\cdot\left(\varepsilon_i\mathbf{v}_i + \frac{P_e\mathbf{v}_e}{\gamma-1} + \mathbf{v}_i\cdot\mathbb{P}_i + \mathbf{v}_e\cdot\mathbb{P}_e + \mathbf{h}_i + \mathbf{h}_e\right) = \mathbf{j}\cdot\mathbf{E}$$

$$+ \mathbf{v}_i\cdot\mathbf{R}_i^{in} + Q_i^{in} - \Gamma_n^{rec}\frac{1}{2}m_i v_i^2 - Q_n^{rec} + \Gamma_i^{ion}(\frac{1}{2}m_i v_n^2 - \phi_{eff}) + Q_i^{ion}$$

$$+ \Gamma^{cx}\frac{1}{2}m_i\left(\mathbf{v}_n^2 - \mathbf{v}_i^2\right) + \mathbf{v}_n\cdot\mathbf{R}_{in}^{cx} - \mathbf{v}_i\cdot\mathbf{R}_{ni}^{cx} + Q_{in}^{cx} - Q_{ni}^{cx}.$$

optically thin radiative losses

The neutral energy equation is

$$\frac{\partial\varepsilon_n}{\partial t} + \nabla\cdot(\varepsilon_n\mathbf{v}_n + \mathbf{v}_n\cdot\mathbb{P}_n + \mathbf{h}_n)$$

$$= -\mathbf{v}_n\cdot\mathbf{R}_i^{in} + Q_n^{ni} - \Gamma_i^{ion}\frac{1}{2}m_i\mathbf{v}_n^2 - Q_i^{ion} + \Gamma_n^{rec}\frac{1}{2}m_i\mathbf{v}_i^2 + Q_n^{rec}$$

$$+ \Gamma^{cx}\frac{1}{2}m_i(\mathbf{v}_i^2 - \mathbf{v}_n^2) + \mathbf{v}_i\cdot\mathbf{R}_{ni}^{cx} - \mathbf{v}_n\cdot\mathbf{R}_{in}^{cx} + Q_{ni}^{cx} - Q_{in}^{cx}.$$

Reacting Multi-Fluid Model in HiFi

Ohm's Law:

We drop the electron inertia and the viscous part of the electron pressure tensor but include electron-neutral collisions as well as electron-ion collisions:

$$\mathbf{E} + (\mathbf{v}_i \times \mathbf{B}) = \eta \mathbf{j} + \frac{\mathbf{j} \times \mathbf{B}}{e n_i} - \frac{1}{e n_i} \nabla P_e - \frac{m_e \nu_{en}}{e} \mathbf{w},$$

"three-fluid" terms accounting for separate electron flow

where $\mathbf{w} = \mathbf{v}_i - \mathbf{v}_n$. The resistivity η is calculated using the electron-ion and electron-neutral collisional frequencies, and thus depends on the plasma conditions:

$$\eta = \frac{m_e n_e (\nu_{ei} + \nu_{en})}{(e n_e)^2}$$

where the electron-ion (ν_{ei}) and electron-neutral (ν_{en}) collision frequencies are given by

$$\nu_{ei} = \frac{4}{3} n_i \Sigma_{ei} \sqrt{\frac{2 k_B T_e}{\pi m_e}}, \text{ and } \nu_{en} = n_n \Sigma_{en} \sqrt{\frac{8 k_B T_{en}}{\pi m_{en}}}.$$